

22 **Abstract**

23 **Background**

24 The lager brewing yeast, *S. pastorianus*, is a hybrid between *S. cerevisiae* and *S. eubayanus* with
25 extensive chromosome aneuploidy. *S. pastorianus* is subdivided into Group 1 and Group 2 strains,
26 where Group 2 strains have higher copy number and a larger degree of heterozygosity for *S.*
27 *cerevisiae* chromosomes. As a result, Group 2 strains were hypothesized to have emerged from a
28 hybridization event distinct from Group 1 strains. Current genome assemblies of *S. pastorianus*
29 strains are incomplete and highly fragmented, limiting our ability to investigate their evolutionary
30 history.

31 **Results**

32 To fill this gap, we generated a chromosome-level genome assembly of the *S. pastorianus* strain CBS
33 1483 using MinION sequencing and analysed the newly assembled subtelomeric regions and
34 chromosome heterozygosity. To analyse the evolutionary history of *S. pastorianus* strains, we
35 developed Alpaca: a method to compute sequence similarity between genomes without assuming
36 linear evolution. Alpaca revealed high similarities between the *S. cerevisiae* subgenomes of Group 1
37 and 2 strains, and marked differences from sequenced *S. cerevisiae* strains.

38 **Conclusions**

39 Our findings suggest that Group 1 and Group 2 strains originated from a single hybridization involving
40 a heterozygous *S. cerevisiae* strain, followed by different evolutionary trajectories. The clear
41 differences between both groups may originate from a severe population bottleneck caused by the
42 isolation of the first pure cultures. Alpaca provides a computationally inexpensive method to analyse
43 evolutionary relationships while considering non-linear evolution such as horizontal gene transfer
44 and sexual reproduction, providing a complementary viewpoint beyond traditional phylogenetic
45 approaches.

46 **Background**

47 The lager-brewing yeast *Saccharomyces pastorianus* is an interspecies hybrid between *S. cerevisiae*
48 and *S. eubayanus*. Lager brewing emerged in the late middle ages and was carried out during winter
49 months at temperatures between 8 and 15 °C, followed by a prolonged maturation period referred
50 to as lagering (1, 2). While *S. cerevisiae* is a well-studied species frequently used in biotechnological
51 processes (3), *S. eubayanus* was only discovered in 2011 and has thus far only been isolated from the
52 wild (4). Therefore, the ancestral *S. pastorianus* hybrid likely emerged from a spontaneous
53 hybridization between an ale brewing *S. cerevisiae* yeast and a wild *S. eubayanus* contaminant, and
54 took over lager brewing due to increased fitness under these conditions (4-6). Indeed, laboratory-
55 made *S. cerevisiae* x *S. eubayanus* hybrids demonstrated hybrid vigour by combining the
56 fermentative capacity and sugar utilisation of *S. cerevisiae* and the ability to grow at lower
57 temperatures of *S. eubayanus* (7, 8).

58 The genomes of *S. pastorianus* strains are highly aneuploid, containing 0 to 5 copies of each
59 chromosome (5, 9-13). Between 45 and 79 individual chromosomes were found in individual *S.*
60 *pastorianus* genomes, compared to a normal complement of 32 chromosomes in euploid
61 *Saccharomyces* hybrids. The degree of aneuploidy of *S. pastorianus* is exceptional in the
62 *Saccharomyces* genera, and likely evolved during its domestication in the brewing environment (9).
63 Nevertheless, two groups can be distinguished based on their genome organisation: Group 1 strains,
64 which have approximately haploid *S. cerevisiae* and diploid *S. eubayanus* chromosome complements;
65 and Group 2 strains, which have approximately diploid to tetraploid *S. cerevisiae* and diploid *S.*
66 *eubayanus* chromosome complements (5, 10, 11, 14).

67 Group 1 and Group 2 strains in *S. pastorianus* were initially thought to have originated from two
68 different hybridization events. Some lager-specific genes from Group 2 strains are absent in Group 1
69 strains, and the subtelomeric regions of Group 1 and Group 2 strains differ substantially (15, 16).
70 Based on these differences, Group 1 and Group 2 strains were hypothesized to have emerged from
71 different independent hybridization events, involving a haploid *S. cerevisiae* for Group 1 strains and a

72 higher ploidy *S. cerevisiae* strain for Group 2 strains (5, 17). Indeed, crosses between *S. cerevisiae* and
73 *S. eubayanus* strains with varying ploidies could be made in the laboratory, all of which performed
74 well in the lager brewing process (18). Comparative genome analysis between Group 1 and Group 2
75 strains revealed that there were more synonymous nucleotide differences in the *S. cerevisiae*
76 subgenome than in the *S. eubayanus* subgenome (19). As accumulation of synonymous mutations
77 was presumed to equally affect both genomes, the authors hypothesized that Group 1 and 2 strains
78 originated from two hybridizations, with a similar *S. eubayanus* parent and different *S. cerevisiae*
79 parents.

80 More recent studies now support that Group 1 and Group 2 strains originated from the same
81 hybridization event. Identical recombinations between the *S. cerevisiae* and *S. eubayanus*
82 subgenomes were found at the *ZUO1*, *MAT*, *HSP82* and *XRN1/KEM1* loci in all analysed *S. pastorianus*
83 strains (11, 13, 14), which did not emerge when such hybrids were evolved under laboratory
84 conditions (20). These conserved recombinations indicate that all *S. pastorianus* strains share a
85 common *S. cerevisiae* x *S. eubayanus* hybrid ancestor, and that the differences between Group 1 and
86 Group 2 strains emerged subsequently. Sequence analysis of ten *S. pastorianus* genomes revealed
87 that the *S. cerevisiae* sub-genome in Group 1 strains is relatively homozygous, while Group 2 strains
88 possess heterozygous sub-regions (11). Moreover, heterozygous nucleotide stretches in Group 2
89 strains were composed of sequences highly similar to Group 1 genomes and of sequences from a
90 different *S. cerevisiae* genome with a 0.5% lower sequence identity. As a result, the authors
91 formulated two hypotheses to explain the emergence of Group 1 and Group 2 strains from a shared
92 ancestral hybrid: (i) the ancestral hybrid had a heterozygous *S. cerevisiae* sub-genome, and Group 1
93 strains underwent a massive reduction of the *S. cerevisiae* genome content while Group 2 did not, or
94 (ii) the ancestral hybrid had a homozygous Group 1-like genome and Group 2 strains were formed by
95 a subsequent hybridization event of such a Group 1-like strain with another *S. cerevisiae* strain,
96 resulting in a mixed *S. cerevisiae* genome content in Group 2 strains.

97 Since the exact *S. cerevisiae* and *S. eubayanus* ancestors of *S. pastorianus* are not available, the
98 evolutionary history of *S. pastorianus* has so far been based on the sequence analysis using available
99 *S. cerevisiae* and *S. eubayanus* reference genomes (5, 11). However, these reference genomes are
100 not necessarily representative of the original parental genomes of *S. pastorianus*. Although *S.*
101 *pastorianus* genomes are available, they were sequenced with short-read sequencing technology
102 (10-13) preventing assembly of large repetitive stretches of several thousand base pairs, such as TY-
103 elements or paralogous genes often found in *Saccharomyces* genomes (21). The resulting *S.*
104 *pastorianus* genomes assemblies are thus incomplete and fragmented into several hundred or
105 thousand contigs (10-13).

106 Single-molecule sequencing technologies can output reads of several thousand base pairs and span
107 entire repetitive regions, enabling near complete chromosome-level genome assemblies of
108 *Saccharomyces* yeasts (22-27). In addition to the lesser fragmentation, the assembly of regions
109 containing repetitive sequences reveals large numbers of previously unassembled open reading
110 frames, particularly in the sub-telomeric regions of chromosomes (24, 25, 27). Sub-telomeric regions
111 are relatively unstable (28), and therefore contain much of the genetic diversity between different
112 strains (29, 30). In *S. pastorianus*, notable differences were found between the sub-telomeric regions
113 of Group 1 and Group 2 strains (15, 16), which could be used to understand their origin. Moreover,
114 repetitive regions are enriched for genes with functions determining the cell's interaction with its
115 environment, such as nutrient uptake, sugar utilization, inhibitor tolerance and flocculation (31-34).
116 As a result, the completeness of sub-telomeric regions is critical for understanding genetic variation
117 and evolutionary relationships between strains, as well as for understanding their performance in
118 industrial applications (24, 29, 30).

119 Here, we used nanopore sequencing to obtain a chromosome-level assembly of the Group 2 *S.*
120 *pastorianus* strain CBS 1483 and analysed the importance of new-found sequences relative to
121 previous genome assemblies, with particular focus on industrially-relevant subtelomeric gene

122 families. As the CBS 1483 genome contains multiple non-identical copies for many chromosomes, we
123 analysed structural and sequence-level heterozygosity using short- and long-read data. Moreover, we
124 developed a method to investigate the evolutionary origin of *S. pastorianus* by evaluating the
125 genome similarity of several Group 1 and Group 2 *S. pastorianus* strains relative to a large dataset of
126 *S. cerevisiae* and *S. eubayanus* genomes, including an isolate of the Heineken A-yeast® lineage which
127 was isolated by dr. Elion in 1886 and is still used in beer production today.

128 **Results**

129 **Near-complete haploid assembly of CBS 1483**

130 We obtained 3.3 Gbp of whole genome sequencing data of the *Saccharomyces pastorianus* strain CBS
131 1483 using 4 flow cells on Oxford Nanopore Technology's MinION platform. Based on a genome size
132 of 46 Mbp accounting for all chromosome copy numbers, the combined coverage was 72x with an
133 average read length of 7 Kbp (Figure S1). We assembled the reads using Canu (35) and performed
134 manual curation involving circularization of the mitochondrial DNA, scaffolding of ScXII (chromosome
135 XII of the *S. cerevisiae* sub-genome) and resolution of assembly problems due to inter- and intra-
136 chromosomal structural heterozygosity in ScI and ScXIV (Figure 1). Assembly errors were corrected
137 with Pilon (36) using paired-end Illumina reads with 159x coverage. We obtained a final assembly of
138 29 chromosome contigs, 2 chromosome scaffolds, and the complete mitochondrial contig leading to
139 a total size of 23.0 Mbp (Figure 2 and Table 1). The assembly was remarkably complete: of the 31
140 chromosomes (in CBS 1483 ScIII and SeIII recombined into a chimeric SeIII-ScIII chromosome(10), 29
141 were in single contigs; 21 of the chromosomes contained both telomere caps; 8 contained one of the
142 caps; and 2 were missing both caps. Some chromosomes contain sequence from both parental sub-
143 genomes due to recombinations; those chromosomes were named SeIII-ScIII, SeVII-ScVII, ScX-ScX,
144 SeX-ScX and SeXIII-ScXIII, in accordance with previous nomenclature (10). Annotation of the assembly
145 resulted in the identification of 10,632 genes (Additional File 1A). We determined chromosome copy

146 number based on coverage analysis of short-read alignments to the genome assembly of CBS 1483
147 (Figure 2 and S2).

148 **Comparison between ONT and Illumina assemblies**

149 In order to compare our novel nanopore assembly of CBS 1483 to the previous assembly generated
150 using short-read data, we aligned contigs of CBS 1483 from van den Broek *et al.* (10) to our current
151 ONT-assembly, revealing a total 1.06 Mbp of added sequence. The added sequence overlapped with
152 323 ORFs (Additional File 1B). Conversely, aligning the nanopore assembly to the van den Broek *et al.*
153 2017 assembly revealed that only 14.9 Kbp of sequence was lost, affecting 15 ORFs (Additional File
154 1C). Gene ontology analysis of the added genes showed enrichment of several biological processes,
155 functions, and components such as flocculation (P-value = 7.44×10^{-3}) as well as transporter activity
156 for several sugars including mannose, fructose and glucose (P-value $\leq 1.5 \times 10^{-5}$) (Additional File 1D).
157 Among the added genes were various members of subtelomeric gene families such as the *FLO*, *SUC*,
158 *MAL*, *HXT* and *IMA* genes (Additional file 1E). Due to their role in the brewing-relevant traits such as
159 carbohydrate utilization and flocculation, the complete assembly of subtelomeric gene families is
160 crucial to capture different gene versions and copy number effects.

161 The assembly of CBS 1483 contained 9 *MAL* transporters, which encode for the ability to import
162 maltose and maltotriose (37-39), constituting 85% of fermentable sugar in brewer's wort (40). The *S.*
163 *cerevisiae* subgenome harboured *ScMAL31* on ScII, *ScMAL11* on ScVII and on SeVII-ScVII, and
164 *ScMAL41* on ScXI (Additional File 1B and 1E). However, the *ScMAL11* gene, also referred to as *AGT1*,
165 was truncated, and there was no *ScMAL21* gene due to the complete absence of ScIII, as reported
166 previously (10, 12). In the *S. eubayanus* subgenome, *MAL31*-type transporter genes were found in
167 *SeII*, *SeV*, and *SeXIII-ScXIII*, corresponding to the location of the *S. eubayanus* transporter genes
168 *SeMALT1*, *SeMALT2* and *SeMALT3*, respectively (25). In addition, a *MAL11*-like transporter was found
169 on *SeXV*. Consistently with previous reports, no *MTY1*-like maltotriose transporter was found in CBS
170 1483 (10). Due to the absence of *MTY1* and the truncation of *ScMAL11*, maltotriose utilisation is

171 likely to rely on the *SeMAL11* transporter in CBS 1483. Indeed, a *MAL11*-like transporter was recently
172 shown to confer maltotriose utilisation in an *S. eubayanus* isolate from North Carolina (41).

173 The assembly also contained 14 *FLO* genes encoding flocculins which cause cell mass sedimentation
174 upon completion of sugar consumption (34, 42, 43). The heavy flocculation of *S. pastorianus* cells
175 simplifies biomass separation at the end of the brewing process, and resulted in their designation as
176 bottom-fermenting yeast (44). Flocculation is mediated by flocculins: lectin-like cell wall proteins
177 which effect cell-to-cell adhesion. In CBS 1483, we identified 12 flocculin genes, in addition to two
178 *FLO8* transcriptional activators of flocculins (Additional File 1E). Flocculation intensity has been
179 correlated to the length of flocculin genes (45-47). Specifically, increased length and number of
180 tandem repeats within the *FLO* genes caused increased flocculation (47, 48). We therefore analysed
181 tandem repeats in *S. cerevisiae*, *S. eubayanus* and *S. pastorianus* genomes and found that most *FLO*
182 genes contain a distinct repeat pattern: two distinct, adjacent sequences each with variable copy
183 number (Table 2). The repeats in *FLO1*, *FLO5*, and *FLO9* of the *S. cerevisiae* strain S288C have the
184 same repeats of 135 bp and 15 bp; while repeats are of 189 bp and 15 bp for *FLO10* and of 132 bp
185 and 45 bp for *FLO11*. The same repeat structures can be found in the *S. eubayanus* strain CBS 12357
186 as *FLO1*, *FLO5*, and *FLO9* contain repeats of 156 and 30 bp; although we were unable to find clear
187 repeat patterns for *FLO10* and *FLO11* in this genome. In *S. pastorianus* CBS 1483, the repeat lengths
188 of *FLO* genes corresponded to the subgenome they were localized in (Table 2). Compared to the non-
189 flocculent S288C and CBS 12357 strains, *FLO* genes were systematically shorter in CBS 1483,
190 contrasting with available theory (42-50). The intense flocculation phenotype of *S. pastorianus* was
191 previously attributed to a gene referred to as *LgFLO1* (49, 51, 52). However, alignment of previously
192 published partial and complete *LgFLO1* sequences did not confirm the presence of a similar ORF in
193 CBS 1483. Moreover, the annotated *FLO* genes had higher identity with *S. eubayanus* and *S.*
194 *cerevisiae* *FLO* genes, than with *LgFLO1*. Therefore, flocculation is likely to rely on one or several of
195 the identified *FLO* genes from *S. cerevisiae* or *S. eubayanus* subgenomes (Table 2).

196 **Sequence heterogeneity in CBS 1483**

197 As other Group 2 *S. pastorianus* strains, CBS 1483 displays heterozygosity between different copies of
198 its *S. cerevisiae* subgenome (11). We therefore systematically identified heterozygous nucleotides in
199 its genome and investigated the ORFs with allelic variation. Using 156x coverage of paired-end
200 Illumina library of CBS 1483, we found a total of 6,367 heterozygous SNPs across the genome
201 (Additional File 1F). Although the heterozygous SNPs are present across the whole genome, they
202 affect primarily the *S. cerevisiae* sub-genome, with the majority clustered around centromeres
203 (Figure 2). Of these positions, 58% were located within ORFs, resulting in 896 ORFs with allelic
204 variation consisting of 1 to 30 heterozygous nucleotides. A total of 685 ORFs showed heterozygosity
205 which would result in amino acid sequence changes, including 16 premature stop codons, 4 lost stop
206 codons and 1566 amino acid substitutions (Additional File 1F). Gene ontology analysis of the ORFs
207 affected by heterozygous calls revealed no significant enrichment in processes, functions of
208 compartments. However, it should be noted that several industrially-relevant genes encoded more
209 than one protein version, such as: the *BDH1* and *BDH2* genes, encoding butane-diol dehydrogenases
210 involved in reduction of the off flavour compound diacetyl (53), the *FLO5* and *FLO9* genes encoding
211 flocculins (50), and the *OAF1* gene encoding a regulator of ethyl-ester production pathway (54).

212 **Structural heterogeneity in CBS 1483 chromosomes**

213 We investigated whether information about structural heterogeneity between chromosome copies
214 could be recovered despite the fact that current assembly algorithms reduce genome assemblies to
215 consensus sequences. Information about structural and sequence variation between different
216 chromosome haplotypes is not captured by consensus assemblies. However, raw read data contains
217 information for each chromosome copy. To identify structural heterogeneity, we identified ORFs
218 whose predicted copy number deviated from that of the surrounding region in the chromosome
219 based on read coverage analysis (Figure S3). We found 213 ORFs with deviating copy number
220 (Additional File 1G). While no enrichment was found by gene ontology analysis, many of these ORFs

221 are located in subtelomeric regions (29). Nevertheless, a few regions contained adjacent ORFs with
222 deviating copy number, indicating larger structural variation between chromosome copies. For
223 example, 21 consecutive ORFs in the right-end of the ScXV appear to have been deleted in 2 of the 3
224 chromosome copies (Figure S3). *UIP3*, one of the genes with deviating copy number, was located on
225 the right arm of chromosome ScI. This region was previously identified as having an additional copy
226 in CBS 1483, although it could not be localized based on short read data (10). The assembly graph
227 showed two possible structures for ScI, which were collapsed into a single contig in the final
228 assembly (Figure 1A). Sequence alignment, gene annotations and sequencing coverage indicated two
229 versions of the ScI contigs: one with and one without the gene *UIP3* (Figure 1B). Sequence alignments
230 of raw-ONT reads revealed five reads (from 20.6 to 36.7 Kbp) linking the right arm of ScI to the left
231 arm of ScXIV at position ~561 Kbp (Figure 1C). This location corresponded to a Ty-2 repetitive
232 element; known to mediate recombination within *Saccharomyces* genomes (21). In addition to the
233 increased coverage of the right arm of ScI, the left arm of ScXIV showed decreased sequencing
234 coverage up until the ~561 Kbp position. Together, these results suggest that the left arm of one
235 copy of ScXIV was replaced with an additional copy of the right arm of ScI (Figure 1D). As no reads
236 covered both the recombination locus and the *UIP3* locus, it remained unclear if *UIP3* is present in
237 the ScI copy translocated to chromosome ScXIV. The resolution of two alternative chromosome
238 architectures of ScI and ScXIV illustrates the ability of long-read alignment to resolve structural
239 heterozygosity.

240 **Differences between Group 1 and 2 genomes do not result from separate** 241 **ancestry**

242 *S. pastorianus* strains can be subdivided into two separate groups—termed Group 1 and Group 2—
243 based on both phenotypic (55) and genomic features (5, 11). However, the ancestral origin of each
244 group remains unclear. The two groups may have emerged by independent hybridization events (19).
245 Alternatively, Group 1 and Group 2 strains may originate from the same hybridization event, but

246 Group 2 strains later hybridized with a different *S. cerevisiae* strain (11). In both cases, analysis of the
247 provenance of genomic material from Group 1 and Group 2 genomes could confirm the existence of
248 separate hybridization events if different ancestries are identified. Pan-genomic analysis of *S.*
249 *cerevisiae* strains indicated that their evolution was largely non-linear, involving frequent horizontal
250 gene transfer and sexual backcrossing events (56). Especially if the evolutionary ancestry of *S.*
251 *pastorianus* involves admixture of different *S. cerevisiae* genomes (11), approaches considering only
252 linear evolution such as phylogenetic trees are insufficient (57). Complex, non-linear evolutionary
253 relationships could be addressed with network approaches (58). However, such algorithms are not
254 yet fully mature and would involve extreme computational challenges (59, 60).

255 Therefore, we developed Alpaca: a simple and computationally inexpensive method to investigate
256 complex non-linear ancestry via comparison of sequencing datasets (61). Alpaca is based on short-
257 read alignment of a collection of strains to a partitioned reference genome, in which the similarity of
258 each partition to the collection of strains is independently computed using k-mer sets (61). Reducing
259 the alignments in each partition to k-mer sets prior to similarity analysis is computationally
260 inexpensive. Phylogenetic relationships are also not recalculated, but simply inferred from previously
261 available information on the population structure of the collection of strains (61). The partitioning of
262 the reference genome enables the identification of strains with high similarity to different regions of
263 the genome, enabling the identification of ancestry resulting from non-linear evolution. Moreover,
264 since similarity analysis is based on read data, heterozygosity is taken into account.

265 We used Alpaca to identify the most similar lineages for all non-overlapping 2 Kbp sub-regions in the
266 genome of the Group 2 *S. pastorianus* strain CBS 1483 using a reference dataset of 157 *S. cerevisiae*
267 strains (62) and 29 *S. eubayanus* strains (63). We inferred population structures for both reference
268 datasets by using previously defined lineages of each strain along with hierarchical clustering based
269 on genome similarity using MASH (64). For the *S. eubayanus* subgenome, almost all sub-regions of
270 CBS 1483 were most similar to strains from the Patagonia B - Holartic lineage (63) (Figure 3). In fact,

271 68% of all sub-regions were most similar to the Tibetan isolate CDFM21L.1 (65) and 27% to two
272 highly-related North-American isolates (Figure 4), indicating a monophyletic ancestry of the *S.*
273 *eubayanus* genome. Analysis of *S. pastorianus* strains CBS 2156 and WS 34/70 (Group2), and of CBS
274 1503, CBS 1513 and CBS 1538 (Group 1), indicated identical ancestry of their *S. eubayanus*
275 subgenomes (Figure 4). Overall, we did not discern differences in the *S. eubayanus* subgenomes of *S.*
276 *pastorianus* strains, which seem to descend from a strain of the Patagonia B – Holartic lineage and
277 which is most closely related to the Tibetan isolate CDFM21L.1.

278 In contrast, for the *S. cerevisiae* sub-genome of CBS 1483, the most similar *S. cerevisiae* strains varied
279 across the sub-regions of every chromosome (Figure 5). No strain of the reference dataset was most
280 similar for more than 5% of sub-regions, suggesting a high degree of admixture (Figure 6). However,
281 60% of sub-regions were most similar to the Beer 1 lineage, 12% were most similar to the Wine
282 lineage and 10% to the Beer 2 lineage (62). In order to determine Alpaca's ability to differentiate
283 genomes with different admixed ancestries, we analysed the genomes of 8 *S. cerevisiae* strains: six
284 ale-brewing strains and the laboratory strains CEN.PK113-7D and S288C. The strains CBS 7539, CBS
285 1463 and A81062 were identified as similar to the Beer 2 lineage, CBS 1171 and CBS 6308 as similar
286 to the Beer 1 lineage, CBS 1487 as similar to the Wine lineage, and CEN.PK113-7D and S288C as
287 similar to the mosaic laboratory strains (Figure 5). In addition, the distribution of similarity over the *S.*
288 *cerevisiae* population tree differed per strain (Figure 6 and S4). While no single strain was most
289 similar for more than 8% of the sub-regions for CBS 1487 and CBS 6308, for CBS 7539 67% of sub-
290 regions were most similar to the strain beer002. As both beer002 and CBS 7539 are annotated as
291 Bulgarian beer yeast (56, 62), this similarity likely reflects common origin. The different similarity
292 profiles of all *S. cerevisiae* strains indicate that Alpaca can differentiate different ancestry by
293 placement of genetic material within the *S. cerevisiae* population tree, whether a genome has a
294 linear monophyletic origin or a non-linear polyphyletic origin.

295 To identify possible differences in genome compositions within the *S. cerevisiae* subgenomes of *S.*
296 *pastorianus*, we analysed other Group 1 and 2 strains using Alpaca, including an isolate of the
297 Heineken A-yeast[®] lineage (Hei-A), which was isolated in 1886 and represents one of the earliest
298 pure yeast cultures. Whole genome sequencing, alignment to the CBS 1483 assembly and sequencing
299 coverage analysis revealed that the ploidy of the Hei-A isolate corresponds to that of a Group 2 strain
300 (Figure S5). Analysis of Hei-A and the other *S. pastorianus* Group 2 strains CBS 2156 and WS 34/70
301 using Alpaca yielded almost identical patterns of similarity at the chromosome-level as CBS 1483
302 (Figure 5). Moreover, similarity was distributed across the *S. cerevisiae* population tree almost
303 identically as in CBS 1483 (Figure 6 and S4). The Group 1 *S. pastorianus* strains CBS 1503, CBS 1513
304 and CBS 1538 displayed different patterns of similarity at the chromosome-level relative to Group 2
305 strains. While various chromosome regions harboured almost identical similarity patterns, some
306 regions differed significantly, such as: ScI, the middle of ScIV, the left arm of ScV, ScVIII, the right arm
307 of ScIX, ScX-ScX, ScXI and ScXIII (Figure 5). However, at the genome level, similarity was distributed
308 across the *S. cerevisiae* population tree almost identically as in Group 2 strains, except for a slightly
309 higher contribution of the Beer 2 and Wine lineages, at the expense of a lower contribution of the
310 Beer 1 lineage (Figure 6 and S4). The almost identical distribution of all Group 1 and Group 2 strains
311 over the *S. cerevisiae* population tree indicate that they have the same *S. cerevisiae* ancestry. The
312 spread of similarity across the *S. cerevisiae* population tree advocates for an admixed, possibly
313 heterozygous ancestry of the *S. cerevisiae* subgenome of *S. pastorianus*. Furthermore, the different
314 patterns of similarity at the chromosome level between both groups are compatible with an initially
315 heterozygous *S. cerevisiae* subgenome which was subjected to independent loss of heterozygosity
316 events in each group, resulting in differential retention of each haplotype. The lower relative
317 contribution of Beer 1 strains in Group 1 strains may be explained by the complete absence of *S.*
318 *cerevisiae* chromosomes with high similarity to Beer1 strains, such as ScV, ScXI and ScXv-ScXI.

319

320 Discussion

321 In this study, we used Oxford Nanopore Technology's (ONT) MinION sequencing platform to study
322 the genome of CBS 1483, an alloaneuploid Group 2 *S. pastorianus* strain. The presence of extensively
323 aneuploid *S. cerevisiae* and *S. eubayanus* subgenomes substantially complicates analysis of *S.*
324 *pastorianus* genomes (10). We therefore explored the ability of nanopore sequencing to generate a
325 reference genome in the presence of multiple non-identical chromosome copies, and investigated
326 the extent to which structural and sequence heterogeneity can be reconstructed. Despite its
327 aneuploidy, we obtained a chromosome-level genome haploid assembly of CBS 1483 in which 29 of
328 the 31 chromosomes were assembled in a single contig. Comparably to assemblies of euploid
329 *Saccharomyces* genomes (22-27), nanopore sequencing resulted in far lesser fragmentation and in
330 the addition of considerable sequences compared to a short-read based assembly of CBS 1483,
331 notably in the subtelomeric regions (10). The added sequences enabled more complete identification
332 of industrially-relevant subtelomeric genes such as the *MAL* genes, responsible for maltose and
333 maltotriose utilisation (37-39), and the *FLO* genes, responsible for flocculation (34, 42, 43). Due to
334 the instability of subtelomeric regions (28-30), the lack of reference-based biases introduced by
335 scaffolding allows more certainty about chromosome structure (24). Since subtelomeric genes
336 encode various industrially-relevant traits (31-34), their mapping enables further progress in strain
337 improvement of lager brewing yeasts. Combined with recently developed Cas9 gene editing tools for
338 *S. pastorianus* (66), accurate localisation and sequence information about subtelomeric genes is
339 critical to investigate their contribution to brewing phenotypes by enabling functional
340 characterization (67).

341 Despite the presence of non-identical chromosome copies in CBS 1483, the genome assembly only
342 contained one contig per chromosome. While the assembly did not capture information about
343 heterogeneity, mapping of short-read data enabled identification of sequence heterozygosity across
344 the whole genome. In previous work, two alternative chromosome structures could be resolved

345 within a population of euploid *S. cerevisiae* strain CEN.PK113-7D by alignment of nanopore reads
346 (24). Therefore, we evaluated the ability to identify structural heterogeneity by aligning nanopore
347 read data to the assembly. Indeed, nanopore-read alignments enabled the identification of two
348 versions of chromosome ScI: with and without an internal deletion of the gene *UIP3*. Furthermore,
349 the length of nanopore reads enabled them to span a TY-element, revealing that one of the copies of
350 the right arm of ScI was translocated to the left arm of ScXIV. While the two alternative structures of
351 ScI constitute a first step towards the generation of chromosome copy haplotypes, nanopore reads
352 only enabled the hypothesis-based resolution of suspected heterogeneity. Assembly algorithms
353 which do not generate a single consensus sequence per chromosome are emerging (68, 69).
354 However, haplotyping is particularly difficult in aneuploid and polyploid genomes due to copy
355 number differences between chromosomes (68). A further reduction of the relatively high error rate
356 of nanopore reads, or the use of more accurate long-read sequencing technologies, could simplify
357 the generation of haplotype-level genome assemblies in the future by reducing noise (70).

358 We used the chromosome-level assembly of CBS 1483 to study the ancestry of *S. pastorianus*
359 genomes. Due to the importance of non-linear evolution in the domestication process of
360 *Saccharomyces* strains (56), and to the admixed hybrid nature of *S. pastorianus* (11, 63), we used the
361 newly-developed method Alpaca to analyse the ancestry of CBS 1483 instead of classical
362 phylogenetic approaches using reference datasets of *S. cerevisiae* and *S. eubayanus* strains (62, 63).
363 All *S. pastorianus* genomes displayed identical distribution of similarity across the reference *S.*
364 *eubayanus* population tree, both at the chromosome and whole-genome level. All *S. pastorianus*
365 genomes also showed identical distribution of similarity across the reference *S. cerevisiae* population
366 tree at the whole genome level; however, Group 1 and Group 2 strains displayed different similarity
367 patterns at the chromosome level. The absence of differences in the *S. cerevisiae* genome at the
368 whole genome level and recurrence of identical chromosomal break points between Group 1 and 2
369 strains discredit previous hypotheses of different independent hybridization events in the evolution
370 of Group 1 and 2 strains (11, 19). Instead, these results are compatible with the emergence of Group

371 1 and 2 strains from a single shared hybridization event between a homozygous *S. eubayanus*
372 genome closely related to the Tibetan isolate CDFM21L.1 and an admixed heterozygous *S. cerevisiae*
373 genome with a complex polyphyletic ancestry. Loss of heterozygosity is frequently observed in
374 *Saccharomyces* genomes (56, 71), and therefore likely to have affected both the genomes of Group 1
375 and 2 strains (11, 72, 73). The different chromosome-level similarity patterns in both groups likely
376 emerged through different loss of heterozygosity events in Group 1 and 2 strains (72, 73). In
377 addition, the lower *S. cerevisiae* chromosome content of Group 1 is consistent with observed loss of
378 genetic material from the least adapted parent during laboratory evolution of *Saccharomyces* hybrids
379 (74-77). In this context, the lower *S. cerevisiae* genome content of Group 1 strains may have resulted
380 from a rare and serendipitous event. For example, chromosome loss has been observed due to
381 unequal chromosome distribution from a sporulation event of a allopolyploid *Saccharomyces* strain
382 (78). Such mutant may have been successful if loss of *S. cerevisiae* chromosomes provided a selective
383 advantage in the low-temperature lager brewing environment (74, 75). The loss of the *S. cerevisiae*
384 subgenome may have affected only Group 1 strains due to different brewing conditions during their
385 domestication. However, the high conservation of similarity within Group 1 and Group 2 strains
386 indicate that the strains within each Group are closely related, indicating a strong population
387 bottleneck in their evolutionary history.

388 Such a bottleneck could have been caused by the isolation and propagation of a limited number *S.*
389 *pastorianus* strains, which may have eventually resulted in the extinction of other lineages. The first
390 *S. pastorianus* strains isolated in 1883 by Hansen at the Carlsberg brewery were all Group 1 strains
391 (13, 79). Due to the industry practice of adopting brewing methods and brewing strains from
392 successful breweries, Hansen's Group 1 isolates likely spread to other breweries as these adopted
393 pure culture brewing (1). Many strains which were identified as Group 2 by whole genome
394 sequencing were isolated in the Netherlands (5, 11): Elion isolated the Heineken A-yeast® in 1886
395 (80), CBS 1484 was isolated in 1925 from the Oranjeboom brewery (5), CBS 1483 was isolated in 1927
396 in a Heineken brewery (10), and CBS 1260, CBS 2156 and CBS 5832 were isolated from unknown

397 breweries in the Netherlands in 1937, 1955 and 1968, respectively (5, 81). Analogously to the spread
398 of Group 1 strains from Hansen's isolate, Group 2 strains may have spread from Elion's isolate. Both
399 Heineken and Carlsberg distributed their pure culture yeast biomass to breweries over Europe and
400 might therefore have functioned as an evolutionary bottleneck by supplanting other lineages with
401 their isolates (82, 83). Overall, our results support that the differences between Group 1 and 2 strains
402 emerged by differential evolution after an initial shared hybridization event, and not by a different *S.*
403 *eubayanus* and/or *S. cerevisiae* ancestry.

404 Beyond its application in this study, we introduced Alpaca as a method to evaluate non-linear
405 evolutionary ancestry. The use of short-read alignments enables Alpaca to account for sequence
406 heterozygosity when assessing similarity between two genomes and is computationally inexpensive
407 as they are reduced to k-mer sets. Moreover, Alpaca leverages previously determined phylogenetic
408 relationships within the reference dataset of strains to infer the evolutionary relationship of the
409 reference genome to the dataset of strains. Due to the presence of non-linear evolutionary processes
410 in a wide range of organisms (84, 85), the applicability of Alpaca extends far beyond the
411 *Saccharomyces* genera. For example, genetic introgressions from *Homo neanderthalensis* constitute
412 about 1% of the human genome (86). Horizontal gene transfer is even relevant across different
413 domains of life: more than 20% of ORFs of the extremely thermophilic bacteria *Thermotoga maritima*
414 were more closely related to genomes of Archaea than to genomes of other Bacteria (87). Critically,
415 horizontal gene transfer, backcrossing and hybridization have not only played a prominent role in the
416 domestication of *Saccharomyces* yeasts (56), but also in other domesticated species such as cows,
417 pigs, wheat and citrus fruits (88-91). Overall, Alpaca can significantly simplify the analysis of new
418 genomes in a broad range of contexts when reference phylogenies are already available.

419 **Conclusions**

420 With 29 of the 31 chromosomes assembled in single contigs and 323 previously unassembled genes,
421 the genome assembly of CBS 1483 presents the first chromosome-level assembly of a *S. pastorianus*

422 strain specifically, and of an alloaneuploid genome in general. While the assembly only consisted of
423 consensus sequences of all copies of each chromosome, sequence and structural heterozygosity
424 could be recovered by alignment of short and long-reads to the assembly, respectively. We
425 developed Alpaca to investigate the ancestry of Group 1 and Group 2 *S. pastorianus* strains by
426 computing similarity between short-read data from *S. pastorianus* strains relative to large datasets of
427 *S. cerevisiae* and *S. eubayanus* strains. In contrast with the hypothesis of separate hybridization
428 events, Group 1 and 2 strains shared similarity with the same reference *S. cerevisiae* and *S.*
429 *eubayanus* strains, indicating shared ancestry. Instead, differences between Group 1 and Group 2
430 strains could be attributed to different patterns of loss of heterozygosity subsequent to a shared
431 hybridization event between a homozygous *S. eubayanus* genome closely related to the Tibetan
432 isolate CDFM21L.1 and an admixed heterozygous *S. cerevisiae* genome with a complex polyphyletic
433 ancestry. We identified the Heineken A-yeast® isolate as a Group 2 strain. We hypothesize that the
434 large differences between Group 1 and Group 2 strains and the high similarity within Group 1 and 2
435 strains result from a strong population bottleneck which occurred during the isolation of the first
436 Group 1 and Group 2 strains, from which all currently known *S. pastorianus* strains descend. Beyond
437 its application in this study, the ability of Alpaca to reveal non-linear ancestry without requiring
438 heavy computations presents a promising alternative to phylogenetic network analysis to investigate
439 horizontal gene transfer, backcrossing and hybridization.

440 **Methods**

441 **Yeast strains, cultivation techniques and genomic DNA extraction**

442 *Saccharomyces* strains used in this study are indicated in Table 3. *S. pastorianus* strain CBS 1483,
443 *S. cerevisiae* strain S288C and *S. eubayanus* strain CBS 12357 were obtained from the Westerdijk
444 Fungal Biodiversity Institute (<http://www.westerdijkinstituut.nl/>). *S. eubayanus* strain
445 CDFM21L.1 was provided by Prof. Feng-Yan Bai. An isolate from the *S. pastorianus* Heineken A-

446 yeast[®] lineage (Hei-A) was obtained from HEINEKEN Supply Chain B.V., Zoeterwoude, the
447 Netherlands. All strains were stored at -80°C in 30% glycerol (vol/vol). Yeast cultures were
448 inoculated from frozen stocks into 500-mL shake flasks containing 100 mL liquid YPD medium
449 (containing 10 g L⁻¹ yeast extract, 20 g L⁻¹ peptone and 20 g L⁻¹ glucose) and incubated at 12 °C on
450 an orbital shaker set at 200 rpm until the strains reached stationary phase with an OD₆₆₀
451 between 12 and 20. Genomic DNA was isolated using the Qiagen 100/G kit (Qiagen, Hilden,
452 Germany) according to the manufacturer's instructions and quantified using a Qubit[®]
453 Fluorometer 2.0 (ThermoFisher Scientific, Waltham, MA).

454 **Short-read Illumina sequencing**

455 Genomic DNA of CBS 1483 and CDFM21L.1 was sequenced on a HiSeq2500 sequencer (Illumina, San
456 Diego, CA) with 125 bp paired-end reads with an insert size of 550 bp using PCR-free library
457 preparation by Keygene (Wageningen, The Netherlands). Genomic DNA of the Heineken A-yeast[®]
458 isolate Hei-A was sequenced in house on a MiSeq sequencer (Illumina) with 300 bp paired-end reads
459 using PCR-free library preparation. All Illumina sequencing data are available at NCBI
460 (<https://www.ncbi.nlm.nih.gov/>) under the bioproject accession number PRJNA522669.

461 **MinION sequencing and basecalling**

462 A total of four MinION genomic libraries of CBS 1483 were created using different chemistries and
463 flow cells: one library using 2D-ligation (Sequencing Kit SQK-MAP006) with a R7.3 chemistry flow cell
464 (FLO-MIN103); two libraries using 2D-ligation (Sequencing Kit SQK-NSK007) with two R9 chemistry
465 flow cells (FLO-MIN105); and one library using 1D-ligation (Sequencing Kit SQK-LASK108) with a R9
466 chemistry flow cell (FLO-MIN106). All libraries were constructed using the same settings as previously
467 described (24) and reads were uploaded and basecalled using the Metrichor desktop agent
468 (<https://metrichor.com/s/>). All nanopore sequencing data are available at NCBI
469 (<https://www.ncbi.nlm.nih.gov/>) under the bioproject accession number PRJNA522669.

470 ***De novo* genome assembly**

471 The genome of CBS 1483 was assembled *de novo* using only the ONT sequencing data generated in
472 this study. The assembly was generated using Canu (35), polished using Pilon (36) and annotated
473 using MAKER2 (92), as previously described (24) with some modifications: Pilon (version 1.22) was
474 only used to polish sequencing errors in the ONT-only *de novo* assembly, and Minimap2 (93) (version
475 2.7) was used as the long-read aligner to identify potential misassemblies and heterozygous
476 structural variants, which were visualized using Ribbon (94). The resulting assembly was manually
477 curated: (i) a contig of 24 Kbp comprised entirely of “TATATA” sequence was discarded; (ii) three
478 contigs of 592, 465, and 95 Kbp (corresponding to the rDNA locus of the *S. cerevisiae* sub-genome)
479 and complete sequence up and downstream of this locus were joined with a gap; (iii) four contigs
480 corresponding to *S. cerevisiae* chromosome I (referred to as ScI) were joined without a gap into a
481 complete 208 Kbp chromosome assembly (Figure 2A); (iv) two contigs corresponding to ScXIV were
482 joined with a gap (Figure 2D); and (v) 23 Kbp of overlapping sequence from the mitochondrial contig
483 corresponding to the origin of replication was identified with Nucmer (95) and manually removed
484 when circularizing the contig, leading to the complete a final size of 69 Kbp. The assembled genomes
485 are available at NCBI (<https://www.ncbi.nlm.nih.gov/>) under the bioproject accession number
486 PRJNA522669. Gene annotations are available in Additional File 1A.

487 **Comparison between ONT-only and Illumina-only genome assembly**

488 Gained and lost sequence information in the nanopore assembly of CBS 1483 was determined by
489 comparing it to the previous short-read assembly (10), as previously described (24) with the addition
490 of using minimum added sequence length of 25 nt.

491 **FLO gene analysis**

492 We used Tandem Repeat Finder (version 4.09) (96) with recommended parameters to identify
493 tandem repeat sequences in *FLO1* (SGDID:S000000084), *FLO5* (SGDID:S000001254), *FLO8*
494 (SGDID:S000000911), *FLO9* (SGDID:S000000059), *FLO10* (SGDID:S000001810), and *FLO11*

495 (SGDID:S000001458) of *S. cerevisiae* strain S288C (97) as well as in *FLO1*, *FLO5*, *FLO8*, *FLO9*, *FLO10*
496 and *FLO11* of *S. eubayanus* strain CBS 12357 (25). The resulting tandem repeat sequences were then
497 used as proxies to characterize *FLO* genes in our assembly of CBS 1483, in a previously generated
498 assembly of *S. cerevisiae* strain CEN.PK113-7D (24) and the *Lg-FLO1* genes previously described in *S.*
499 *cerevisiae* strain CMBSVM11 (GenBank HM358276) and *S. pastorianus* strain KBY001 (GenBank
500 D89860.1) (51, 52). BLASTN (version 2.2.31+) (98) was then used to align the tandem sequences to
501 each *FLO* gene. The alignments were further processed via an in-house script in the Scala
502 programming language to identify repeat clusters by requiring a minimum alignment coverage of 0.5
503 and a maximum gap between two repeats of 3x times the repeat sequence length. The total number
504 of copies was estimated by dividing the total size of the cluster by the repeat sequence length.

505 **Intra-chromosomal heterozygosity**

506 Sequence variation was identified by aligning the short-read Illumina reads generated in this study to
507 the ONT-only assembly with BWA (99) and calling variants with Pilon (36) using the `--fix "bases"`,
508 `"local"` and `--diploid` parameters. To restrict false positive calls, SNPs were disregarded within 10 Kbp
509 of the ends of the chromosomes, if minor alleles had a frequency below 15% allele frequency, and if
510 the coverage was below 3 reads.

511 Copy number variation for all chromosomes were estimated by aligning all short-reads to the ONT-
512 only assembly. Reads were trimmed of adapter sequences and low-quality bases with Trimmomatic
513 (100) (version 0.36) and aligned with BWA (99) (version 0.7.12). The median coverage was computed
514 using a non-overlapping window of 100 nt, copy number was determined by comparing the coverage
515 to that of the chromosome with the smallest median coverage. Additionally, copy number variation
516 at the gene-level was also investigated based on whether the coverage of an individual gene
517 significantly deviated from the coverage of the surrounding region. First, we defined contiguous
518 chromosomal sub-regions with fixed copy number (Table S1). The mean and standard deviation of
519 coverages of these sub-regions were then computed using ONT-only alignments. Mean coverages of

520 every gene was then computed and an uncorrected Z-test (101) was performed by comparing a
521 gene's mean coverage and the corresponding mean and standard deviation of the pre-defined sub-
522 region that the gene overlapped with.

523 **Similarity analysis and lineage tracing of *S. pastorianus* sub-genomes using** 524 **Alpaca**

525 We developed Alpaca (61) to investigate non-linear ancestry of a reference genome based on large
526 sequencing datasets. Briefly, Alpaca partitions a reference genome into multiple sub-regions, each
527 reduced to a k-mer set representation. Sequence similarities of the sub-regions are then
528 independently computed against the corresponding sub-regions in a collection of target genomes.
529 Non-linear ancestry can therefore be inferred by tracing the population origin of the most similar
530 genome(s) in each sub-region. Detailed explanation Alpaca can be found in our method description
531 (61).

532 Alpaca (version 1.0) was applied to the ONT CBS 1483 genome assembly to investigate the similarity
533 of sub-regions from both sub-genomes to previously defined population lineages. For partitioning
534 the CBS 1483 genome into sub-regions, we used a k-mer size of 21 and a sub-region size of 2 Kbp and
535 used the short-read Illumina data of CBS 1483 produced in this study to assure accurate k-mer set
536 construction. For investigating mosaic structures in the *S. cerevisiae* subgenome, we used 157
537 brewing-related *S. cerevisiae* genomes (project accession number PRJNA323691) which were
538 subdivided in six major lineages: Asia, Beer1, Beer2, Mixed, West-Africa, Wine and Mosaic (62). For
539 the *S. eubayanus* subgenome, we used 29 available genomes (project accession number
540 PRJNA290017) which were subdivided in three major lineages: Admixed, Patagonia-A, and Patagonia-
541 B (63). Raw-reads of all samples were trimmed Trimmomatic and filtered reads were aligned to CBS
542 1483 genome using BWA (99). Alpaca was also applied to several *Saccharomyces* genomes to
543 investigate evolutionary similarities and differences between Group 1 and Group 2 *S. pastorianus*
544 genomes. We used Group 1 strains CBS 1503, CBS 1513, and CBS 1538, and Group 2 strains CBS 2156

545 and WS34/70 (project accession number PRJDB4073) (11). As a control, eight *S. cerevisiae* genomes
546 were analysed: ale strains CBS 7539, CBS 1463, CBS 1171, CBS 6308, and CBS 1487 (project accession
547 number PRJEB13017) (56) and A81062 (project accession number PRJNA408119) (18), and laboratory
548 strains CEN.PK113-7D (project accession number PRJNA393501) (24) and S288C (project accession
549 number PRJEB14774) (23). Similarly, raw-reads for all strains were trimmed with Trimmomatic and
550 aligned to the ONT CBS 1483 genome assembly using BWA. Partitioning of the additional *S.*
551 *pastorianus* and *S. cerevisiae* genomes with Alpaca was performed by deriving k-mer sets from read-
552 alignments only, assuring direct one-to-one comparison of all sub-regions across all genomes. K-mer
553 size of 21 and sub-region size of 2 Kbp were used. The *S. cerevisiae* and *S. eubayanus* sequencing
554 data were used to identify potential mosaic structures in these genomes. Lastly, *S. cerevisiae* and *S.*
555 *eubayanus* strains were subdivided into subpopulations according to previously defined lineages (62,
556 63). MASH (version 2.1) (64) was then used to hierarchically cluster each genome based on their
557 MASH distance using k-mer size of 21, sketch size of 1,000,000, and minimum k-mer frequency of 2.
558 The resulting trees were used as population reference trees for Alpaca (61).

559 **Declarations**

560 **Ethics approval and consent to participate**

561 Not applicable

562 **Consent for publication**

563 Not applicable

564 **Availability of data and materials**

565 The datasets generated and/or analysed during the current study are available in the NCBI
566 repository, <https://www.ncbi.nlm.nih.gov/>.

567 **Competing interests**

568 NGAK is an employee of Heineken Supply Chain B.V. The remaining authors declare no conflict of
569 interest.

570 **Funding**

571 BE-Basic R&D Program (<http://www.be-basic.org/>), which was granted a TKI-subsidy subsidy from
572 the Dutch Ministry of Economic Affairs, Agriculture and Innovation (EL&I). Funding for open access
573 charge: BE-Basic.

574 **Authors' contributions**

575 ANS and PdITC performed nanopore sequencing. NB performed illumina sequencing. ANS performed
576 sequence assembly. ANS, ARGDV and MvdB analysed the data. ANS designed and applied Alpaca.
577 HEINEKEN Supply Chain B.V. provided the Heineken A-yeast[®] isolate. NGA supported sequencing and
578 reviewed the manuscript. ANS and ARGDV wrote the manuscript. JMGD and TA supervised the study.
579 All authors read and approved the final manuscript.

580 **Acknowledgments**

581 We thank Prof. Feng Yan Bai for kindly providing us *S. eubayanus* strain CDFM21L.1, as well as Prof.
582 Jack Pronk and Dr. Jan-Maarten Geertman for their support throughout the study.

583 **References**

- 584 1. Meussdoerffer FG. A comprehensive history of beer brewing. In: Eßlinger HM, editor.
585 Handbook of brewing: Processes, technology, markets. Weinheim: Wiley-VCH; 2009. p. 1-42.
- 586 2. Kodama Y, Kielland-Brandt MC, Hansen J. Lager brewing yeast. Comparative genomics.
587 Berlin: Springer; 2006. p. 145-64.
- 588 3. Dequin S. The potential of genetic engineering for improving brewing, wine-making and
589 baking yeasts. Appl Microbiol Biotechnol. 2001;56(5-6):577-88.
- 590 4. Libkind D, Hittinger CT, Valério E, Gonçalves C, Dover J, Johnston M, et al. Microbe
591 domestication and the identification of the wild genetic stock of lager-brewing yeast. Proc Natl Acad
592 Sci U S A. 2011;108(35):14539-44.
- 593 5. Dunn B, Sherlock G. Reconstruction of the genome origins and evolution of the hybrid lager
594 yeast *Saccharomyces pastorianus*. Genome Res. 2008;18(10):1610-23.
- 595 6. de Barros Lopes M, Bellon JR, Shirley NJ, Ganter PF. Evidence for multiple interspecific
596 hybridization in *Saccharomyces sensu stricto* species. FEMS Yeast Res. 2002;1(4):323-31.
- 597 7. Hebly M, Brickwedde A, Bolat I, Driessen MR, de Hulster EA, van den Broek M, et al. *S.*
598 *cerevisiae* × *S. eubayanus* interspecific hybrid, the best of both worlds and beyond. FEMS Yeast Res.
599 2015;15(3).
- 600 8. Krogerus K, Magalhães F, Vidgren V, Gibson B. New lager yeast strains generated by
601 interspecific hybridization. J Ind Microbiol Biotechnol. 2015;42(5):769-78.
- 602 9. Gorter de Vries AR, Pronk JT, Daran J-MG. Industrial relevance of chromosomal copy number
603 variation in *Saccharomyces* yeasts. Appl Environ Microbiol. 2017:AEM. 03206-16.

- 604 10. Van den Broek M, Bolat I, Nijkamp J, Ramos E, Luttik MA, Koopman F, et al. Chromosomal
605 copy number variation in *Saccharomyces pastorianus* evidence for extensive genome dynamics in
606 industrial lager brewing strains. *Appl Environ Microbiol.* 2015;AEM. 01263-15.
- 607 11. Okuno M, Kajitani R, Ryusui R, Morimoto H, Kodama Y, Itoh T. Next-generation sequencing
608 analysis of lager brewing yeast strains reveals the evolutionary history of interspecies hybridization.
609 *DNA Res.* 2016;23(1):67-80.
- 610 12. Nakao Y, Kanamori T, Itoh T, Kodama Y, Rainieri S, Nakamura N, et al. Genome sequence of
611 the lager brewing yeast, an interspecies hybrid. *DNA Res.* 2009;16(2):115-29.
- 612 13. Walther A, Hesselbart A, Wendland J. Genome sequence of *Saccharomyces carlsbergensis*,
613 the world's first pure culture lager yeast. *G3 (Bethesda).* 2014;g3. 113.010090.
- 614 14. Hewitt SK, Donaldson IJ, Lovell SC, Delneri D. Sequencing and characterisation of
615 rearrangements in three *S. pastorianus* strains reveals the presence of chimeric genes and gives
616 evidence of breakpoint reuse. *PLoS One.* 2014;9(3):e92203.
- 617 15. Liti G, Peruffo A, James SA, Roberts IN, Louis EJ. Inferences of evolutionary relationships from
618 a population survey of LTR-retrotransposons and telomeric-associated sequences in the
619 *Saccharomyces sensu stricto* complex. *Yeast.* 2005;22(3):177-92.
- 620 16. Monerawela C, James TC, Wolfe KH, Bond U. Loss of lager specific genes and subtelomeric
621 regions define two different *Saccharomyces cerevisiae* lineages for *Saccharomyces pastorianus* Group
622 I and II strains. *FEMS Yeast Res.* 2015;15(2):fou008.
- 623 17. Rainieri S, Kodama Y, Kaneko Y, Mikata K, Nakao Y, Ashikari T. Pure and mixed genetic lines of
624 *Saccharomyces bayanus* and *Saccharomyces pastorianus* and their contribution to the lager brewing
625 strain genome. *Appl Environ Microbiol.* 2006;72(6):3968-74.
- 626 18. Krogerus K, Arvas M, De Chiara M, Magalhães F, Mattinen L, Oja M, et al. Ploidy influences
627 the functional attributes of *de novo* lager yeast hybrids. *Appl Microbiol Biotechnol.*
628 2016;100(16):7203-22.
- 629 19. Baker E, Wang B, Bellora N, Peris D, Hulfachor AB, Koshalek JA, et al. The genome sequence
630 of *Saccharomyces eubayanus* and the domestication of lager-brewing yeasts. *Mol Biol Evol.*
631 2015;32(11):2818-31.
- 632 20. Gorter de Vries A, Voskamp MA, van Aalst ACA, Kristensen LH, Jansen L, van den Broek M, et
633 al. Laboratory evolution of a *Saccharomyces cerevisiae* x *S. eubayanus* hybrid under simulated lager-
634 brewing conditions: genetic diversity and phenotypic convergence. *bioRxiv.* 2018.
- 635 21. Kim JM, Vanguri S, Boeke JD, Gabriel A, Voytas DF. Transposable elements and genome
636 organization: a comprehensive survey of retrotransposons revealed by the complete *Saccharomyces*
637 *cerevisiae* genome sequence. *Genome Res.* 1998;8(5):464-78.
- 638 22. Giordano F, Aigrain L, Quail MA, Coupland P, Bonfield JK, Davies RM, et al. *De novo* yeast
639 genome assemblies from MinION, PacBio and MiSeq platforms. *Sci Rep.* 2017;7(1):3935.
- 640 23. Istace B, Friedrich A, d'Agata L, Faye S, Payen E, Beluche O, et al. *de novo* assembly and
641 population genomic survey of natural yeast isolates with the Oxford Nanopore MinION sequencer.
642 *Gigascience.* 2017;6(2):1-13.
- 643 24. Salazar AN, Gorter de Vries AR, van den Broek M, Wijsman M, de la Torre Cortés P,
644 Brickwedde A, et al. Nanopore sequencing enables near-complete *de novo* assembly of
645 *Saccharomyces cerevisiae* reference strain CEN. PK113-7D. *FEMS Yeast Res.* 2017;17(7).
- 646 25. Brickwedde A, Brouwers N, van den Broek M, Gallego Murillo JS, Fraiture JL, Pronk JT, et al.
647 Structural, physiological and regulatory analysis of maltose transporter genes in *Saccharomyces*
648 *eubayanus* CBS 12357T. *Front Microbiol.* 2018;9:1786.
- 649 26. Yue J-X, Li J, Aigrain L, Hallin J, Persson K, Oliver K, et al. Contrasting evolutionary genome
650 dynamics between domesticated and wild yeasts. *Nat Genet.* 2017;49(6):913.
- 651 27. McIlwain SJ, Peris D, Sardi M, Moskvin OV, Zhan F, Myers K, et al. Genome sequence and
652 analysis of a stress-tolerant, wild-derived strain of *Saccharomyces cerevisiae* used in biofuels
653 research. *G3 (Bethesda).* 2016;g3. 116.029389.

- 654 28. Pryde FE, Huckle TC, Louis EJ. Sequence analysis of the right end of chromosome XV in
655 *Saccharomyces cerevisiae*: an insight into the structural and functional significance of sub-telomeric
656 repeat sequences. *Yeast*. 1995;11(4):371-82.
- 657 29. Bergström A, Simpson JT, Salinas F, Barré B, Parts L, Zia A, et al. A high-definition view of
658 functional genetic variation from natural yeast genomes. *Mol Biol Evol*. 2014;31(4):872-88.
- 659 30. Brown CA, Murray AW, Verstrepen KJ. Rapid expansion and functional divergence of
660 subtelomeric gene families in yeasts. *Curr Biol*. 2010;20(10):895-903.
- 661 31. Jordan P, Choe J-Y, Boles E, Oreb M. Hxt13, Hxt15, Hxt16 and Hxt17 from *Saccharomyces*
662 *cerevisiae* represent a novel type of polyol transporters. *Sci Rep*. 2016;6:23502.
- 663 32. Teste M-A, François JM, Parrou J-L. Characterization of a new multigene family encoding
664 isomaltases in the yeast *Saccharomyces Cerevisiae*: the *IMA* family. *J Biol Chem*. 2010;jbc. M110.
665 145946.
- 666 33. Denayrolles M, de Villechenon EP, Lonvaud-Funel A, Aigle M. Incidence of *SUC-RTM*
667 telomeric repeated genes in brewing and wild wine strains of *Saccharomyces*. *Curr Genet*.
668 1997;31(6):457-61.
- 669 34. Teunissen A, Steensma H. The dominant flocculation genes of *Saccharomyces cerevisiae*
670 constitute a new subtelomeric gene family. *Yeast*. 1995;11(11):1001-13.
- 671 35. Koren S, Walenz BP, Berlin K, Miller JR, Bergman NH, Phillippy AM. Canu: scalable and
672 accurate long-read assembly via adaptive k-mer weighting and repeat separation. *Genome Res*.
673 2017;gr. 215087.116.
- 674 36. Walker BJ, Abeel T, Shea T, Priest M, Abouelliel A, Sakthikumar S, et al. Pilon: an integrated
675 tool for comprehensive microbial variant detection and genome assembly improvement. *PLoS One*.
676 2014;9(11):e112963.
- 677 37. Alves SL, Herberts RA, Hollatz C, Trichez D, Miletti LC, De Araujo PS, et al. Molecular analysis
678 of maltotriose active transport and fermentation by *Saccharomyces cerevisiae* reveals a determinant
679 role for the *AGT1* permease. *Appl Environ Microbiol*. 2008;74(5):1494-501.
- 680 38. Chang Y, Dubin R, Perkins E, Michels C, Needleman R. Identification and characterization of
681 the maltose permease in genetically defined *Saccharomyces* strain. *J Bacteriol*. 1989;171(11):6148-
682 54.
- 683 39. Naumov GI, Naumova ES, Michels C. Genetic variation of the repeated *MAL* loci in natural
684 populations of *Saccharomyces cerevisiae* and *Saccharomyces paradoxus*. *Genetics*. 1994;136(3):803-
685 12.
- 686 40. Zastrow C, Hollatz C, De Araujo P, Stambuk B. Maltotriose fermentation by *Saccharomyces*
687 *cerevisiae*. *J Ind Microbiol Biotechnol*. 2001;27(1):34-8.
- 688 41. Baker EP, Hittinger CT. Evolution of a novel chimeric maltotriose transporter in
689 *Saccharomyces eubayanus* from parent proteins unable to perform this function. *bioRxiv*. 2018.
- 690 42. Van Mulders SE, Christianen E, Saerens SM, Daenen L, Verbelen PJ, Willaert R, et al.
691 Phenotypic diversity of Flo protein family-mediated adhesion in *Saccharomyces cerevisiae*. *FEMS*
692 *Yeast Res*. 2009;9(2):178-90.
- 693 43. Miki B, Poon NH, James AP, Seligy VL. Possible mechanism for flocculation interactions
694 governed by gene *FLO1* in *Saccharomyces cerevisiae*. *J Bacteriol*. 1982;150(2):878-89.
- 695 44. Dengis PB, Nelissen L, Rouxhet PG. Mechanisms of yeast flocculation: comparison of top-and
696 bottom-fermenting strains. *Appl Environ Microbiol*. 1995;61(2):718-28.
- 697 45. Fidalgo M, Barrales RR, Jimenez J. Coding repeat instability in the *FLO11* gene of
698 *Saccharomyces yeasts*. *Yeast*. 2008;25(12):879-89.
- 699 46. Zara G, Zara S, Pinna C, Marceddu S, Budroni M. *FLO11* gene length and transcriptional level
700 affect biofilm-forming ability of wild flor strains of *Saccharomyces cerevisiae*. *Microbiology*.
701 2009;155(12):3838-46.
- 702 47. Verstrepen KJ, Jansen A, Lewitter F, Fink GR. Intragenic tandem repeats generate functional
703 variability. *Nat Genet*. 2005;37(9):986.
- 704 48. Liu N, Wang D, Wang ZY, He XP, Zhang B. Genetic basis of flocculation phenotype conversion
705 in *Saccharomyces cerevisiae*. *FEMS Yeast Res*. 2007;7(8):1362-70.

- 706 49. Ogata T, Izumikawa M, Kohno K, Shibata K. Chromosomal location of Lg-*FLO1* in bottom-
707 fermenting yeast and the *FLO5* locus of industrial yeast. *J Appl Microbiol.* 2008;105(4):1186-98.
- 708 50. Soares EV. Flocculation in *Saccharomyces cerevisiae*: a review. *J Appl Microbiol.*
709 2011;110(1):1-18.
- 710 51. Van Mulders SE, Ghequire M, Daenen L, Verbelen PJ, Verstrepen KJ, Delvaux FR. Flocculation
711 gene variability in industrial brewer's yeast strains. *Appl Microbiol Biotechnol.* 2010;88(6):1321-31.
- 712 52. Kobayashi O, Hayashi N, Kuroki R, Sone H. Region of Flo1 proteins responsible for sugar
713 recognition. *J Bacteriol.* 1998;180(24):6503-10.
- 714 53. Li P, Guo X, Shi T, Hu Z, Chen Y, Du L, et al. Reducing diacetyl production of wine by
715 overexpressing *BDH1* and *BDH2* in *Saccharomyces uvarum*. *J Ind Microbiol Biotechnol.*
716 2017;44(11):1541-50.
- 717 54. Saerens S, Thevelein J, Delvaux F. Ethyl ester production during brewery fermentation, a
718 review. *Cerevisia.* 2008;33(2):82-90.
- 719 55. Gibson BR, Storgårds E, Krogerus K, Vidgren V. Comparative physiology and fermentation
720 performance of Saaz and Froberg lager yeast strains and the parental species *Saccharomyces*
721 *eubayanus*. *Yeast.* 2013;30(7):255-66.
- 722 56. Peter J, De Chiara M, Friedrich A, Yue J-X, Pflieger D, Bergström A, et al. Genome evolution
723 across 1,011 *Saccharomyces cerevisiae* isolates. *Nature.* 2018;556(7701):339.
- 724 57. Gogarten JP, Townsend JP. Horizontal gene transfer, genome innovation and evolution. *Nat*
725 *Rev Microbiol.* 2005;3(9):679.
- 726 58. Solís-Lemus C, Bastide P, Ané C. PhyloNetworks: a package for phylogenetic networks. *Mol*
727 *Biol Evol.* 2017;34(12):3292-8.
- 728 59. Hejase HA, Liu KJ. A scalability study of phylogenetic network inference methods using
729 empirical datasets and simulations involving a single reticulation. *BMC bioinformatics.*
730 2016;17(1):422.
- 731 60. Consortium CP-G. Computational pan-genomics: status, promises and challenges. *Brief*
732 *Bioinform.* 2016;19(1):118-35.
- 733 61. Salazar A, Abeel T. Alpaca: a kmer-based approach for investigating mosaic structures in
734 microbial genomes. *bioRxiv.* 2019:551234.
- 735 62. Gallone B, Steensels J, Prah T, Soriaga L, Saels V, Herrera-Malaver B, et al. Domestication and
736 divergence of *Saccharomyces cerevisiae* beer yeasts. *Cell.* 2016;166(6):1397-410. e16.
- 737 63. Peris D, Langdon QK, Moriarty RV, Sylvester K, Bontrager M, Charron G, et al. Complex
738 ancestries of lager-brewing hybrids were shaped by standing variation in the wild yeast
739 *Saccharomyces eubayanus*. *PLoS Genet.* 2016;12(7):e1006155.
- 740 64. Ondov BD, Treangen TJ, Melsted P, Mallonee AB, Bergman NH, Koren S, et al. Mash: fast
741 genome and metagenome distance estimation using MinHash. *Genome Biol.* 2016;17(1):132.
- 742 65. Bing J, Han P-J, Liu W-Q, Wang Q-M, Bai F-Y. Evidence for a Far East Asian origin of lager beer
743 yeast. *Curr Biol.* 2014;24(10):R380-R1.
- 744 66. Gorter de Vries AR, Groot PA, Broek M, Daran J-MG. CRISPR-Cas9 mediated gene deletions in
745 lager yeast *Saccharomyces pastorianus*. *Microb Cell Fact.* 2017;16(1):222.
- 746 67. Winzeler EA, Shoemaker DD, Astromoff A, Liang H, Anderson K, Andre B, et al. Functional
747 characterization of the *S. cerevisiae* genome by gene deletion and parallel analysis. *Science.*
748 1999;285(5429):901-6.
- 749 68. He D, Saha S, Finkers R, Parida L. Efficient algorithms for polyploid haplotype phasing. *BMC*
750 *genomics.* 2018;19(2):110.
- 751 69. Chin C-S, Peluso P, Sedlazeck FJ, Nattestad M, Concepcion GT, Clum A, et al. Phased diploid
752 genome assembly with single-molecule real-time sequencing. *Nat Methods.* 2016;13(12):1050.
- 753 70. Wenger AM, Peluso P, Rowell WJ, Chang P-C, Hall RJ, Concepcion GT, et al. Highly-accurate
754 long-read sequencing improves variant detection and assembly of a human genome. *bioRxiv.*
755 2019:519025.

- 756 71. Magwene PM, Kayıkcı Ö, Granek JA, Reininga JM, Scholl Z, Murray D. Outcrossing, mitotic
757 recombination, and life-history trade-offs shape genome evolution in *Saccharomyces cerevisiae*. Proc
758 Natl Acad Sci U S A. 2011;108(5):1987-92.
- 759 72. Chambers SR, Hunter N, Louis EJ, Borts RH. The mismatch repair system reduces meiotic
760 homeologous recombination and stimulates recombination-dependent chromosome loss. Mol Cell
761 Biol. 1996;16(11):6110-20.
- 762 73. González SS, Barrio E, Querol A. Molecular characterization of new natural hybrids of
763 *Saccharomyces cerevisiae* and *S. kudriavzevii* in brewing. Appl Environ Microbiol. 2008;74(8):2314-20.
- 764 74. Smukowski Heil CS, DeSevo CG, Pai DA, Tucker CM, Hoang ML, Dunham MJ. Loss of
765 heterozygosity drives adaptation in hybrid yeast. Mol Biol Evol. 2017;34(7):1596-612.
- 766 75. Heil CS, Large CR, Patterson K, Dunham MJ. Temperature preference biases parental genome
767 retention during hybrid evolution. bioRxiv. 2018:429803.
- 768 76. Pérez Través L, Lopes CA, Barrio E, Querol A. Study of the stabilization process in
769 *Saccharomyces* intra- and interspecific hybrids in fermentation conditions. Int Microbiol.
770 2014;17(4):213-24.
- 771 77. Antunovics Z, Nguyen H-V, Gaillardin C, Sipiczki M. Gradual genome stabilisation by
772 progressive reduction of the *Saccharomyces uvarum* genome in an interspecific hybrid with
773 *Saccharomyces cerevisiae*. FEMS Yeast Res. 2005;5(12):1141-50.
- 774 78. Lopandic K, Pfliegler WP, Tiefenbrunner W, Gangl H, Sipiczki M, Sterflinger K. Genotypic and
775 phenotypic evolution of yeast interspecies hybrids during high-sugar fermentation. Appl Microbiol
776 Biotechnol. 2016;100(14):6331-43.
- 777 79. Hansen EC. Recherches sur la physiologie et la morphologie des ferments alcooliques. V.
778 Methodes pour obtenir des cultures pures de *Saccharomyces* et de microorganismes analogues.
779 Compt Rend Trav Lab Carlsberg. 1883;2:92-105.
- 780 80. Gélinas P. Mapping early patents on baker's yeast manufacture. Compr Rev Food Sci Food
781 Saf. 2010;9(5):483-97.
- 782 81. Scheda R, Yarrow D. Variation in the fermentative pattern of some *Saccharomyces* species.
783 Arch Mikrobiol. 1968;61(3):310-6.
- 784 82. Hornsey IS. A history of beer and brewing. Cambridge, UK: Royal Society of Chemistry; 2003.
- 785 83. Mendlik F. Some aspects of the scientific development of brewing in Holland. J Inst Brew.
786 1937;43(4):294-300.
- 787 84. Keeling PJ, Palmer JD. Horizontal gene transfer in eukaryotic evolution. Nat Rev Genet.
788 2008;9(8):605.
- 789 85. Thomas CM, Nielsen KM. Mechanisms of, and barriers to, horizontal gene transfer between
790 bacteria. Nat Rev Microbiol. 2005;3(9):711.
- 791 86. Racimo F, Sankararaman S, Nielsen R, Huerta-Sánchez E. Evidence for archaic adaptive
792 introgression in humans. Nat Rev Genet. 2015;16(6):359.
- 793 87. Nelson KE, Clayton RA, Gill SR, Gwinn ML, Dodson RJ, Haft DH, et al. Evidence for lateral gene
794 transfer between Archaea and bacteria from genome sequence of *Thermotoga maritima*. Nature.
795 1999;399(6734):323.
- 796 88. Larson G, Dobney K, Albarella U, Fang M, Matisoo-Smith E, Robins J, et al. Worldwide
797 phylogeography of wild boar reveals multiple centers of pig domestication. Science.
798 2005;307(5715):1618-21.
- 799 89. McTavish EJ, Decker JE, Schnabel RD, Taylor JF, Hillis DM. New World cattle show ancestry
800 from multiple independent domestication events. Proc Natl Acad Sci U S A. 2013;110(15):E1398-
801 E406.
- 802 90. Brenchley R, Spannagl M, Pfeifer M, Barker GL, D'Amore R, Allen AM, et al. Analysis of the
803 bread wheat genome using whole-genome shotgun sequencing. Nature. 2012;491(7426):705.
- 804 91. Wu GA, Prochnik S, Jenkins J, Salse J, Hellsten U, Murat F, et al. Sequencing of diverse
805 mandarin, pummelo and orange genomes reveals complex history of admixture during citrus
806 domestication. Nat Biotechnol. 2014;32(7):656.

- 807 92. Holt C, Yandell M. MAKER2: an annotation pipeline and genome-database management tool
808 for second-generation genome projects. BMC bioinformatics. 2011;12(1):491.
- 809 93. Li H. Minimap2: pairwise alignment for nucleotide sequences. Bioinformatics.
810 2018;34(18):3094-100.
- 811 94. Nattestad M, Chin C-S, Schatz MC. Ribbon: visualizing complex genome alignments and
812 structural variation. bioRxiv. 2016:082123.
- 813 95. Kurtz S, Phillippy A, Delcher AL, Smoot M, Shumway M, Antonescu C, et al. Versatile and
814 open software for comparing large genomes. Genome Biol. 2004;5(2):R12.
- 815 96. Benson G. Tandem repeats finder: a program to analyze DNA sequences. Nucleic acids
816 research. 1999;27(2):573-80.
- 817 97. Cherry JM, Hong EL, Amundsen C, Balakrishnan R, Binkley G, Chan ET, et al. Saccharomyces
818 Genome Database: the genomics resource of budding yeast. Nucleic acids research.
819 2011;40(D1):D700-D5.
- 820 98. Camacho C, Coulouris G, Avagyan V, Ma N, Papadopoulos J, Bealer K, et al. BLAST+:
821 architecture and applications. BMC bioinformatics. 2009;10(1):421.
- 822 99. Li H, Durbin R. Fast and accurate long-read alignment with Burrows–Wheeler transform.
823 Bioinformatics. 2010;26(5):589-95.
- 824 100. Bolger AM, Lohse M, Usadel B. Trimmomatic: a flexible trimmer for Illumina sequence data.
825 Bioinformatics. 2014;30(15):2114-20.
- 826 101. Fisher RA. The design of experiments: Oliver And Boyd; Edinburgh; London; 1937.
- 827 102. Goffeau A, Barrell BG, Bussey H, Davis R, Dujon B, Feldmann H, et al. Life with 6000 genes.
828 Science. 1996;274(5287):546-67.

829 **Figures legends and tables**

830 **Figure 1.** Structural heterozygosity within multiple copies of the *S. cerevisiae* chromosome I of CBS
831 1483. (A) Layout of *S. cerevisiae* chromosome I in the assembly graph. Paths 1 and 2 represent
832 alternative contigs in the right-end of the chromosome—the gene *UIP3* is deleted in path 2. (B)
833 Sequencing coverage of ONT read-alignments of CBS 1483 in the right-end of chromosome I after
834 joining path 1 and discarding path 2. The location of the *UIP3* gene is indicated. (C) Alignment
835 overview of five raw ONT reads supporting the introgression of a ~14 Kbp in chromosome I (salmon
836 colour) to a region at the right-end of chromosome XIV (brown colour) in the *S. cerevisiae* sub-
837 genome. The additional alignments (pink and orange) are alignments to computationally confirmed
838 Ty-2 repetitive elements. (D) Schematic representation of the two chromosome architectures of *S.*
839 *cerevisiae* chromosome XIV (brown colour) due to translocation of an additional copy of the right
840 arm of chromosome I (salmon colour) to the left arm of chromosome XIV.

841 **Figure 2.** Overview of Nanopore-only *de novo* genome assembly of the *S. pastorianus* strain, CBS
842 1483. For each chromosome, all copies are represented. Genomic material originating from *S.*
843 *cerevisiae* (blue) and from *S. eubayanus* (red) are shown, and the position of the centromere is
844 indicated. Heterozygous SNP calls are represented as vertical, black lines and are drawn with
845 transparency to depict the density of SNP calls in a given region. Underlying chromosome copy
846 number data and the list of heterozygous SNPs is available in Figure S2 and Additional File 1F.

847 **Figure 3.** Similarity profiles of the *S. eubayanus* (sub-)genomes of Group 1 and 2 *S. pastorianus*
848 strains, as determined using Alpaca. Each *S. eubayanus* chromosome of the CBS 1483 assembly was
849 partitioned in non-overlapping sub-regions of 2 Kbp. The colors represent the most similar lineages
850 based on k-mer similarity of 29 *S. eubayanus* strains from Peris *et al* (63): admixed (purple),

851 Patagonia-A (red), Patagonia-B (blue). Similarity patterns are shown for the Group 2 strains CBS 1483,
852 CBS 2156 and WS34/70 and the Group 1 strains CBS 1503, CBS 1513 and CBS 1538.

853 **Figure 4.** Tree-tracing of the genome-scale similarity across the *S. eubayanus* (sub-)genomes of
854 Group 1 and 2 *S. pastorianus* strains, as determined using Alpaca. The frequency at which a genome
855 from the reference data set of 29 *S. eubayanus* genomes from Peris *et al* (63) was identified as most
856 similar for a sub-region of the CBS 1483 genome is depicted. The reference dataset is represented as
857 a population tree, upon which only lineages with similarity are indicated with a thickness
858 proportional to the frequency at which they were found as most similar ('N' being the total sum of
859 the number of times all samples appeared as top-scoring). The complete reference population tree
860 (A), the genomes of Group 1 strains CBS 1503, CBS 1513 and CBS 1538 (B-D) and for the genomes of
861 Group 2 strains CBS 1483, CBS 2156 and WS34/70 (E-G) are shown.

862 **Figure 5.** Similarity profiles of the *S. cerevisiae* (sub-)genomes of various *Saccharomyces* strains, as
863 determined using Alpaca. Each *S. cerevisiae* chromosome of the CBS 1483 assembly was partitioned
864 in non-overlapping sub-regions of 2 Kbp. The colors represent the most similar lineages based on k-
865 mer similarity of 157 *S. cerevisiae* strains from Gallone *et al* (62): Asia (blue), Beer1 (green), Beer2,
866 (gold), Mixed (orange), West-Africa (purple), Wine (red). Mosaic strains are shown in black and
867 ambiguous or low-similarity sub-regions in white. Similarity patterns are shown for the Group 2 *S.*
868 *pastorianus* strains CBS 1483, CBS 2156, WS34/70 and Hei-A, for the Group 1 *S. pastorianus* strains
869 CBS 1503, CBS 1513 and CBS 1538, for *S. cerevisiae* ale-brewing strains CBS 7539, CBS 1463, A81062,
870 CBS 1171, CBS 6308 and CBS 1483, and for *S. cerevisiae* laboratory strains CEN.PK113-7D and S288C.

871 **Figure 6.** Tree-tracing of the genome-scale similarity across the *S. cerevisiae* (sub-)genomes of
872 various *Saccharomyces* strains, as determined using Alpaca. The frequency at which a genome from
873 the reference data set of 157 *S. cerevisiae* strains from Gallone *et al* (62) was identified as most
874 similar for a sub-region of the CBS 1483 genome is depicted. The reference dataset is represented as
875 a population tree, upon which only lineages with similarity are indicated with a thickness
876 proportional to the frequency at which they were found as most similar ('n' being the total sum of
877 the number of times all samples appeared as top-scoring). The genomes of *S. pastorianus* Group 1
878 strain CBS 1513 (A), of *S. pastorianus* Group 2 strain CBS 1483 (B), of *S. cerevisiae* strain CBS 7539 and
879 of *S. cerevisiae* strain CBS 1171 are shown. The tree-tracing figures of *S. pastorianus* Group 1 strains
880 CBS 1503 and CBS 1538, of *S. pastorianus* Group 2 strains CBS 2156, WS34/70 and Hei-A, and of *S.*
881 *cerevisiae* strains CBS 1463, A81062, CBS 6308, CBS 1487, CEN.PK113-7D and S288C are shown in
882 Figure S4.

883 **Table 1.** Length and gaps of each assembled chromosome of the *S. cerevisiae* and *S. eubayanus*
 884 subgenome in the *de novo* assembly of Group 2 *S. pastorianus* strain CBS 1483. The mitochondrial
 885 DNA assembly is also shown.

<i>S. cerevisiae</i> sub-genome			<i>S. eubayanus</i> sub-genome		
Contig/Scaffold	Size	Gaps	Contig/Scaffold	Size	Gaps
ScI	208794	0	SeI	183365	0
ScII	812290	0	SeII	1284912	0
ScIII	0	0	SeIII	311639	0
ScIV	1480484	0	SeIV	995872	0
ScV	590259	0	SeV	580717	0
ScVI	263951	0	SeVI	268897	0
ScVII	862436	0	SeVII	1048199	0
ScVIII	547874	0	SeVIII	813607	0
ScIX	426203	0	SeIX	413986	0
ScX	772632	0	SeX	698708	0
ScXI	662864	0	SeXI	658371	0
ScXII	1128411	2	SeXII	1043408	0
ScXIII	872991	0	SeXIII	966749	0
ScXIV	783474	0	SeXIV	765784	1
ScXV	1060500	0	SeXV	754183	0
Sc XVI	926828	0	SeXVI	788293	0
Unplaced	36198	0	Mitochondria	68765	0

886

887 **Table 2.** Tandem repeat analysis in *FLO* genes. We found seven repeat sequences when analysing
 888 flocculation genes *FLO1*, *FLO5*, *FLO9*, *FLO10*, and *FLO11* in *S. cerevisiae* (S288C) and *S. eubayanus*
 889 (CBS 12357) genomes. These sequences are referred to as sequence A (135 nt), B (15 nt), C (189 nt),
 890 D (45 nt), E (132 nt), F (156 nt), and G (30 nt). We used these sequences to analyse the copy numbers
 891 of each repeat within all *FLO* genes in our ONT-only assembly of CBS 1483 using the ONT-only S288C
 892 assembly as a control. Their respective copy numbers are shown below. Repeat sequences are
 893 indicated in Additional File 1H.

Species	(Sub)genome	Gene	Gene size (nt)	A	B	C	D	E	F	G	
<i>S. cerevisiae</i>	S288C	<i>FLO1</i>	4614	18.0	9.4	-	-	-	-	-	
		<i>FLO5</i>	3228	8.0	9.6	-	-	-	-	-	
		<i>FLO9</i>	3969	13.0	8.3	-	-	-	-	-	
		<i>FLO10</i>	3510	-	3.8	4.4	-	-	-	-	
		<i>FLO11</i>	4104	-	-	-	38.7	6.6	-	-	
		S288C (ONT)									
		<i>FLO1</i>	4615	18.0	9.4	-	-	-	-	-	
		<i>FLO5</i>	3228	8.0	9.6	-	-	-	-	-	
		<i>FLO9</i>	3978	13.0	8.3	-	-	-	-	-	
		<i>FLO10</i>	3508	-	3.8	4.4	-	-	-	-	
		<i>FLO11</i>	4104	-	-	-	38.7	6.6	-	-	
		CBS 1483									
		<i>FLO1</i> (ScVI)	1038	-	-	-	-	-	-	-	-
		<i>FLO5</i> (ScI)	2603	1.0	11.1	-	-	-	-	-	-
		<i>FLO9</i> (ScI)	2967	5.0	15.4	-	-	-	-	-	-
		<i>FLO11</i> (ScIX)	2787	-	-	-	14.1	5.6	-	-	-
	<i>S. eubayanus</i>	CBS 12357	<i>FLO1</i>	5517	-	-	-	-	-	24.7	2.8
			<i>FLO5</i>	1325	-	-	-	-	-	-	-
			<i>FLO9</i> (SeI)	4752	-	-	-	-	-	8.3	45.9
<i>FLO9</i> (SeVI)			3480	-	-	-	-	-	-	-	
<i>FLO9</i> (SeX)			4041	-	-	-	-	-	7.4	20.1	
<i>FLO9</i> (SeXII)			3321	-	-	-	-	-	-	10.2	
<i>FLO10</i> (SeXI)			4128	-	-	-	-	-	-	-	
<i>FLO11</i> (SeIX)			4149	-	-	-	-	-	-	-	
		CBS 1483									
		<i>FLO5</i> (SeI)	1945	-	-	-	-	-	4.9	2.8	
		<i>FLO5</i> (SeI)	391	-	-	-	-	-	-	-	
		<i>FLO5</i> (SeVI)	3765	-	-	-	-	-	-	-	
		<i>FLO5</i> (SeXI)	2582	-	-	-	-	-	4.9	2.8	
		<i>FLO9</i> (SeI)	2100	-	-	-	-	-	3.0	3.8	
		<i>FLO9</i> (SeXII)	2892	-	-	-	-	-	-	6.3	
	<i>FLO10</i> (SeVI)	3378	-	-	-	-	-	-	-		
	<i>FLO11</i> (SeIX)	3909	-	-	-	-	-	-	-		

894

895 **Table 3: *Saccharomyces* strains used in this study.** For strains of the reference dataset, please refer
896 to their original publication (62, 63).

Name	Species	Descriptio	Reference
CBS 1483	<i>S. pastorianus</i>	Group 2	(10)
CBS 2156	<i>S. pastorianus</i>	Group 2	(11)
WS 34/70	<i>S. pastorianus</i>	Group 2	(12)
Heineken A-yeast®	<i>S. pastorianus</i>	Group 2	This study
CBS 1503	<i>S. pastorianus</i>	Group 1	(11)
CBS 1513	<i>S. pastorianus</i>	Group 1	(13)
CBS 1538	<i>S. pastorianus</i>	Group 1	(11)
S288C	<i>S. cerevisiae</i>	Laboratory strain	(102)
CEN.PK113-7D	<i>S. cerevisiae</i>	Laboratory strain	(24)
CBS 7539	<i>S. cerevisiae</i>	Ale brewing strain	(56)
CBS 1463	<i>S. cerevisiae</i>	Ale brewing strain	(56)
A81062	<i>S. cerevisiae</i>	Ale brewing strain	(18)
CBS 1171	<i>S. cerevisiae</i>	Ale brewing strain	(56)
CBS 6308	<i>S. cerevisiae</i>	Ale brewing strain	(56)
CBS 1487	<i>S. cerevisiae</i>	Ale brewing strain	(56)
CBS 12357	<i>S. eubayanus</i>	Patagonian Isolate	(4)
CDFM21L.1	<i>S. eubayanus</i>	Tibetan isolate	(65)

897 Supplemental file, figure and table legends

898 **Additional File 1A:** Gene annotations of the nanopore assembly of CBS 1483 as predicted by
899 MAKER2.

900 **Additional File 1B:** Added sequence in the nanopore assembly relative to the van den Broek et al
901 2015 assembly.

902 **Additional File 1C:** Lost sequence in the nanopore assembly relative to the van den Broek et al 2015
903 assembly.

904 **Additional File 1D:** Gene ontology analysis of genes identified in the nanopore assembly which were
905 absent in the van den Broek et al 2015 assembly.

906 **Additional file 1E:** Genes from brewing-relevant subtelomeric gene families in the nanopore
907 assembly of CBS 1483

908 **Additional file 1F:** Heterozygous sequences in the nanopore assembly of CBS 1483

909 **Additional file 1G:** ORFs with copy number deviating from the copy number of surrounding
910 sequences in the nanopore assembly of CBS 1483

911 **Additional File 1H:** Sequences of the repeats identified in FLO genes of *S. cerevisiae* S288C and *S.*
912 *eubayanus* CBS 12357.

913 **Figure S1.** Read-length distribution obtained of the MinION libraries of CBS 1483 produced in this
914 study. This plot shows the four different sequencing libraries obtained from whole genome
915 sequencing of CBS 1483 using the MinION® platform. The Y-axis is the frequency and the X-axis depicts
916 read-lengths (capped at 30 Kbp) using bins of 500 bp. The libraries were obtained with different
917 sequencing chemistries due to the rapid development of Nanopore sequencing.

918 **Figure S2.** The ploidy estimates for each chromosome in the CBS 1483 assembly based on Illumina
919 short read data from this study. The red horizontal lines correspond to the median coverage of each
920 chromosome.

921 **Figure S3.** Copy number predictions for ORFs in the genome assembly of CBS 1483. Each dot
922 represents an ORF whose x-value represents the location in the corresponding chromosome and the
923 y-value the estimated copy number based on coverage analysis of ONT-only read alignments. Dots in
924 yellow indicate ORFs whose coverage significantly deviates from the surrounding genomic region,
925 indicating copy number variation of the ORF within different copies of the same chromosome.

926 **Figure S4.** More complete version of the tree tracing of Figure 6. Tree-tracing of the genome-scale
927 similarity across the *S. cerevisiae* (sub-)genomes of various *Saccharomyces* strains, as determined
928 using Alpaca. The frequency at which a genome from the reference data set of 157 *S. cerevisiae*
929 strains from Gallone *et al* (62) was identified as most similar for a sub-region of the CBS 1483
930 genome is depicted. The reference dataset is represented as a population tree, upon which only
931 lineages with similarity are indicated with a thickness proportional to the frequency at which they
932 were found as most similar. In addition to the genomes of CBS 1513, CBS 1483, CBS 7539 and CBS
933 1171, the tree-tracing figures of *S. pastorianus* Group 1 strains CBS 1503 and CBS 1538, of *S.*

934 *pastorianus* Group 2 strains CBS 2156, WS34/70 and Hei-A, and of *S. cerevisiae* strains CBS 1463,
935 A81062, CBS 6308, CBS 1487, CEN.PK113-7D and S288C are shown.

936 **Figure S5.** The ploidy estimates for each chromosome of the *S. pastorianus* isolate of the Heineken A-
937 yeast® lineage based on alignment of short-read data to the chromosome-level assembly of CBS
938 1483.

939 **Table S1.** Contiguous sub-regions in the CBS 1483 genome with fixed copy number.

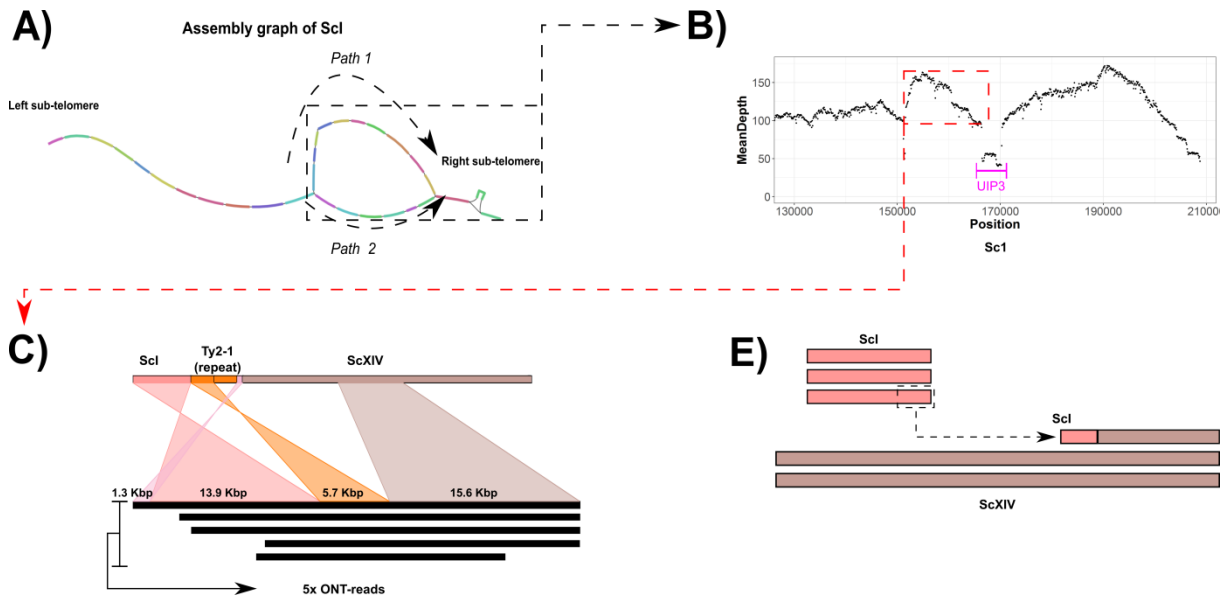
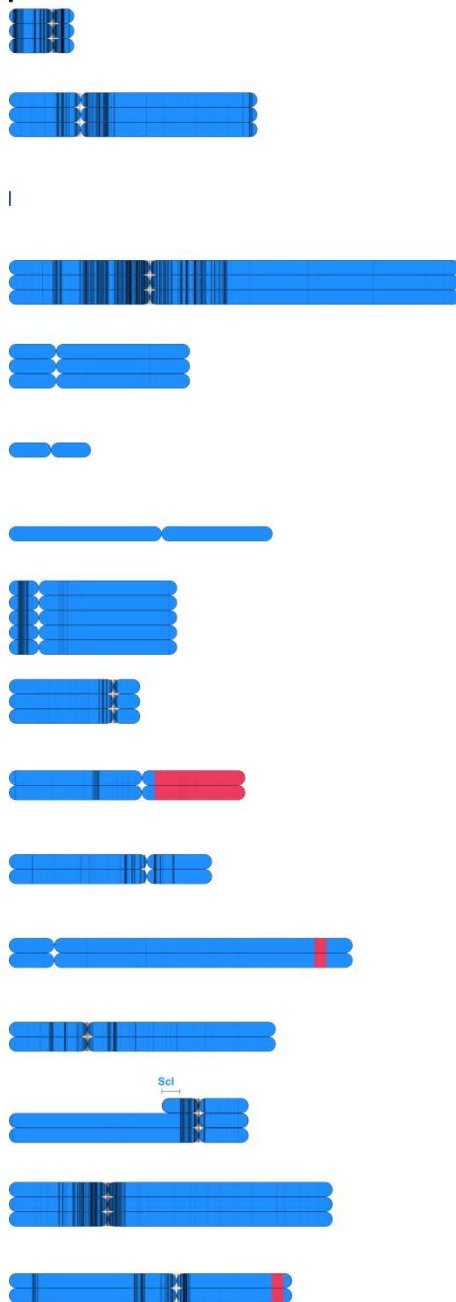


Figure 1. Structural heterozygosity within multiple copies of the *S. cerevisiae* chromosome I of CBS 1483.

S.cerevisiae sub-genome

max size = 1.48 Mbp



S.eubayanus sub-genome

max size = 1.28 Mbp

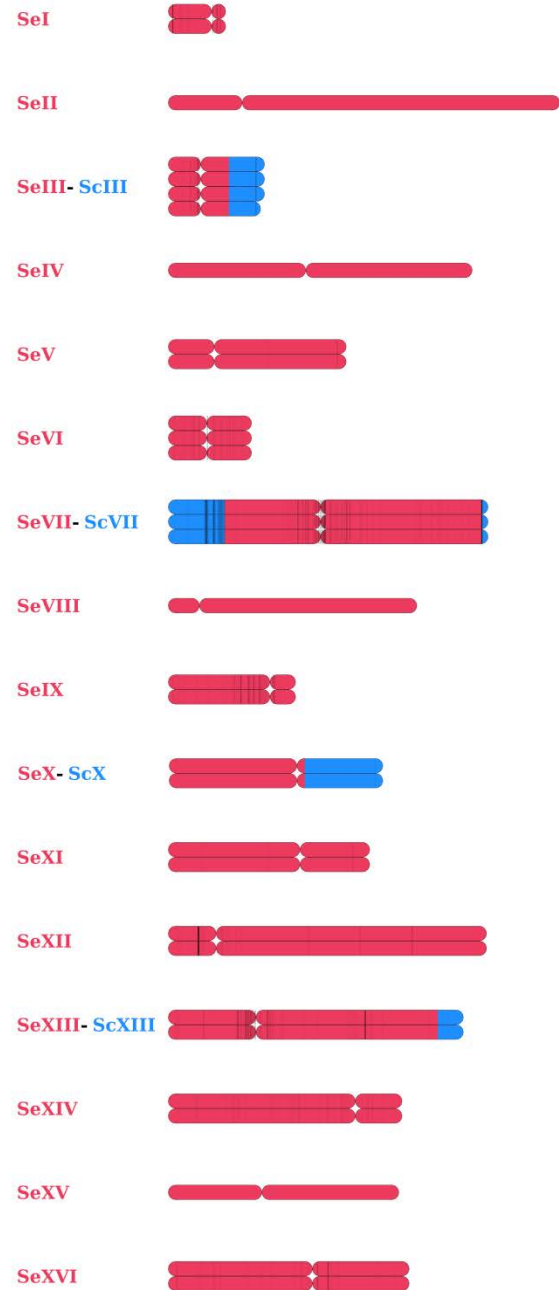


Figure 2. Overview of Nanopore-only *de novo* genome assembly of the *S. pastorianus* strain, CBS 1483.

Lineages
Admixed
Patagonia-A
Patagonia-B

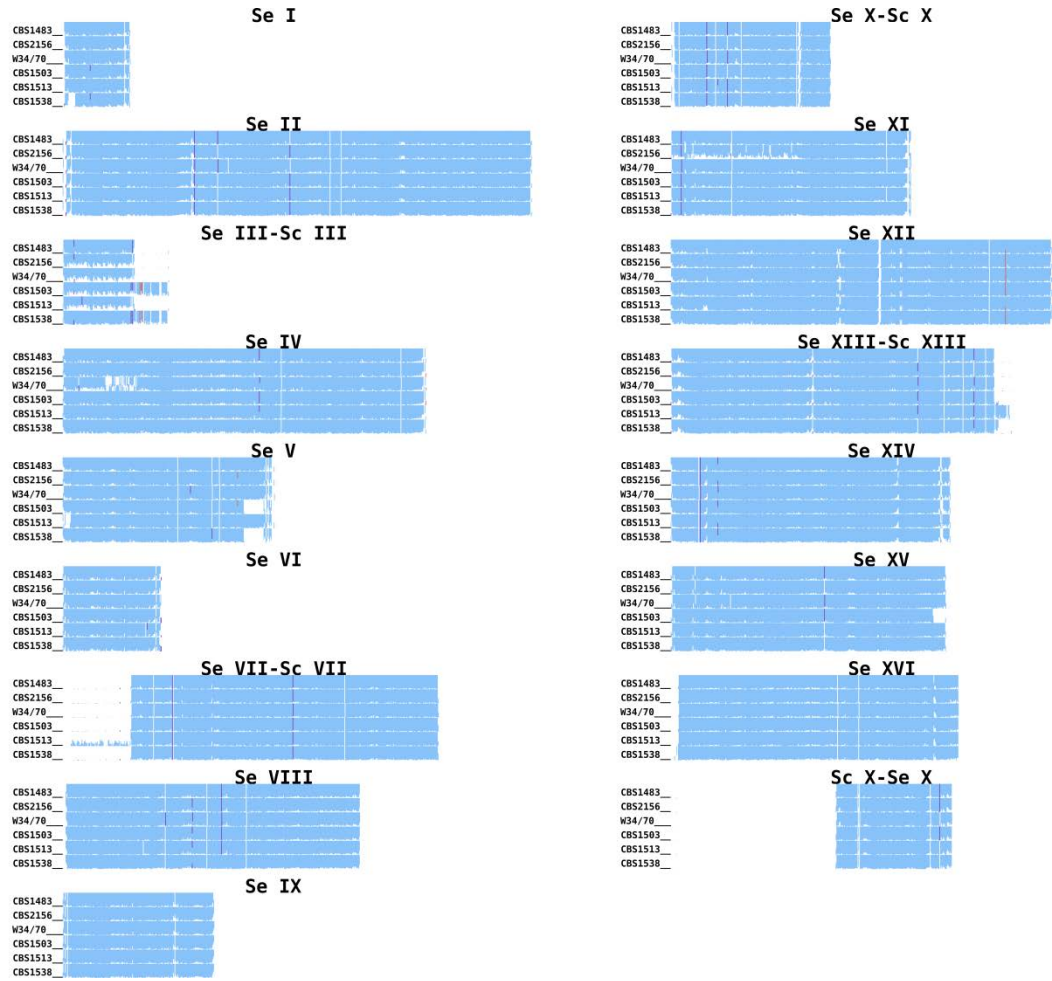


Figure 3. Similarity profiles of the *S. eubayanus* (sub-)genomes of Group 1 and 2 *S. pastorianus* strains, as determined using Alpaca.

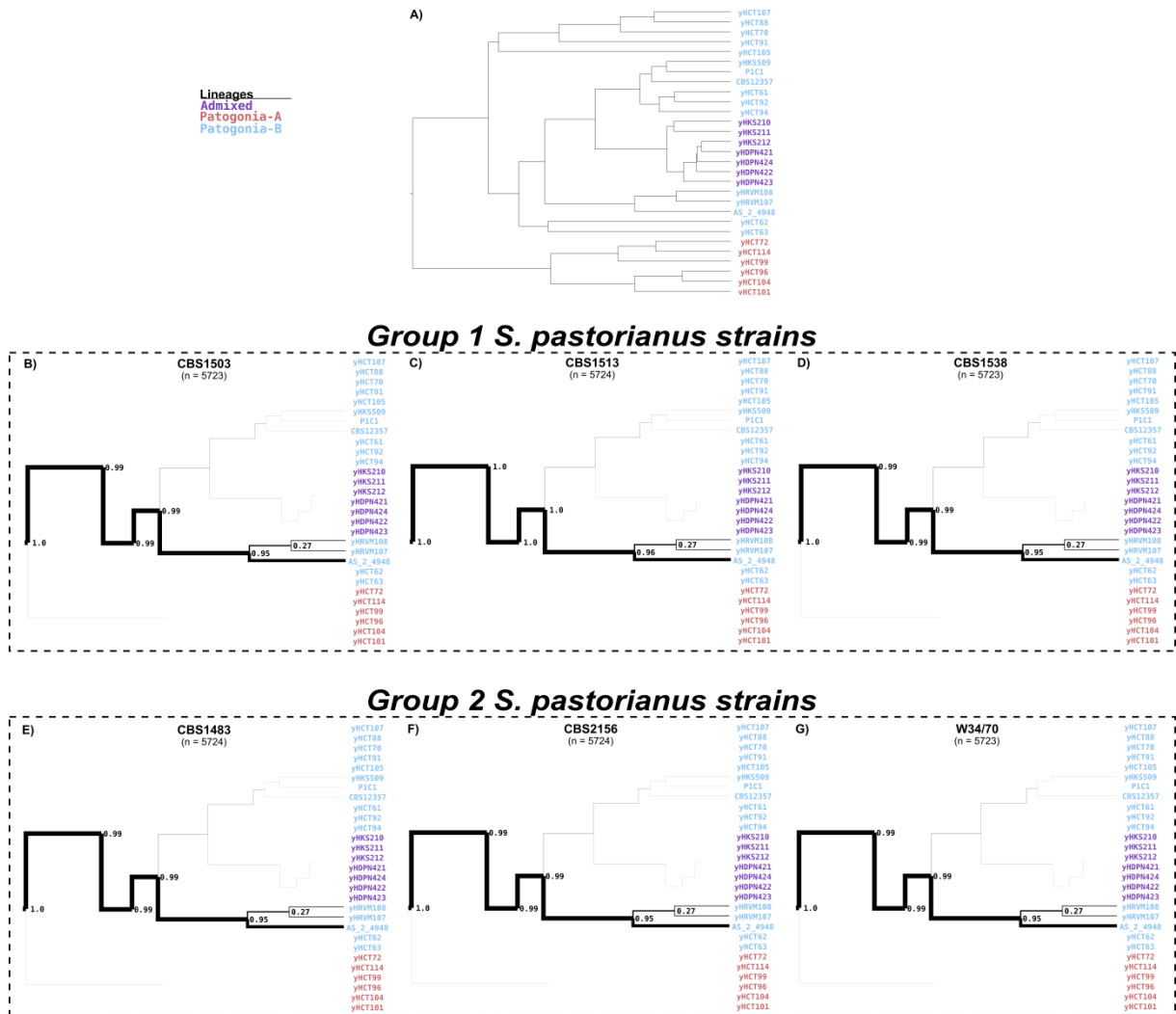


Figure 4. Tree-tracing of the genome-scale similarity across the *S. eubayanus* (sub-)genomes of Group 1 and 2 *S. pastorianus* strains, as determined using Alpacca.

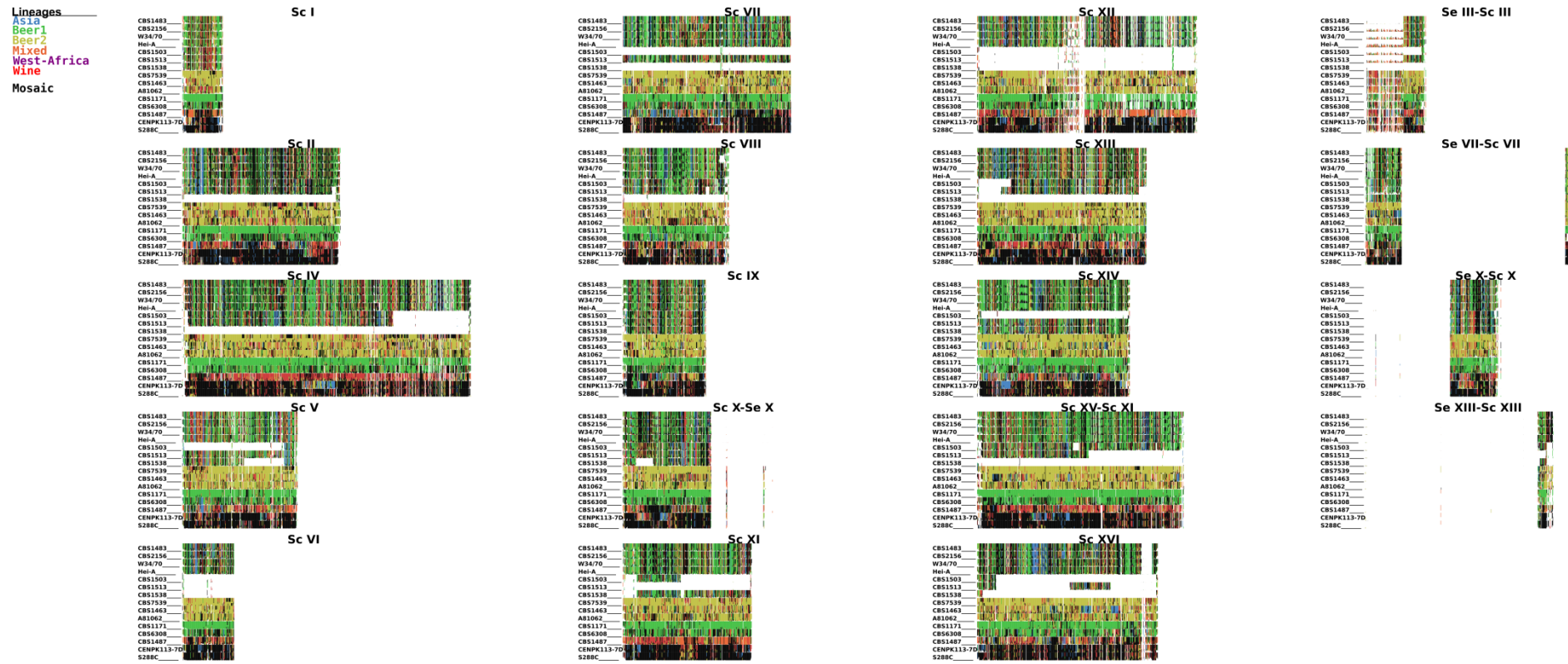


Figure 5. Similarity profiles of the *S. cerevisiae* (sub-)genomes of various *Saccharomyces* strains, as determined using Alpaca.

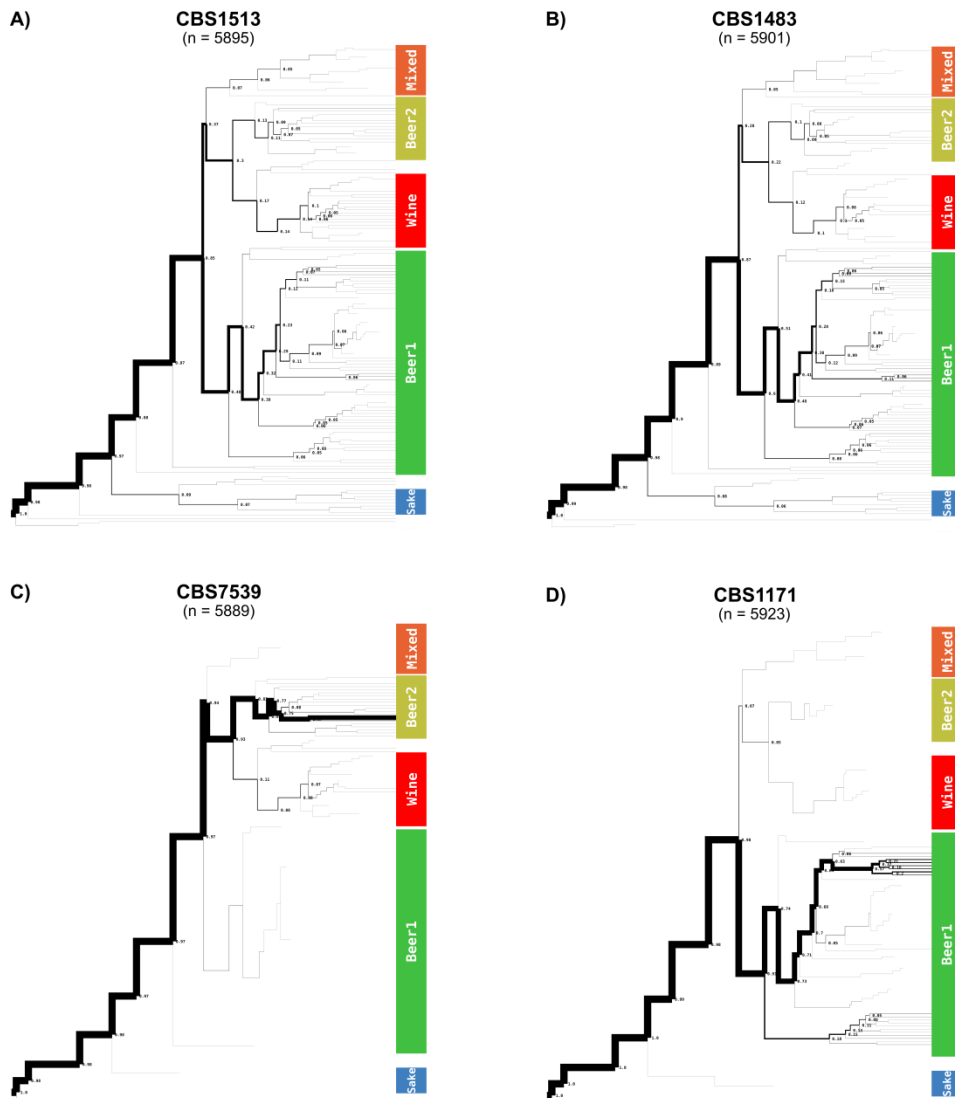


Figure 6. Tree-tracing of the genome-scale similarity across the *S. cerevisiae* (sub-)genomes of various *Saccharomyces* strains, as determined using Alpaca.